SPATIAL-TEMPORAL STRUCTURE OF FLUCTUATIONS OF THE AMPLITUDE AND PHASE OF ACOUSTICAL WAVE PROPAGATING THROUGH THE ATMOSPHERIC BOUNDARY LAYER

Final Technical Report

by

Nikolai Petrovich Krasnenko

(September 1998)

United States Army
EUROPEAN RESEARCH OFFICE OF THE U.S.ARMY
London England

CONTRACT NUMBER 68171-96-C-9067

Institute of Atmospheric Optics,
Siberian Branch of the Russian Academy of Sciences

Approved for public release; distribution unlimited

REPORT DOCUMENTATION PAGE		Form Approved OMB No. 0704-0188

1. AGENCY USE ONLY (Leave blank)	2. REPORT DATE	3.REPORT TYPE AND DATES COVERED
	September 1998	Final, 6 Aug. 1996 to 1 Sept. 1998

4. TITLE AND SUBTITLE
Spatial-temporal sructure of fluctuations of the amplitude and phase of acoustical wave propagating through the atmospheric boundary layer

5. FUNDING NUMBERS
C N 68171-96-C-9067

6. AUTHOR(S)
N.P. Krasnenko, A.L. Afanas'ev, A.Ya.Bogushevich, L.G.Shamanaeva, A.P.Rostov, O.A.Rubtsova

7. PERFORMING ORGANIZATION NAME (S) and ADRESS(ES)
Institute of Atmospheric Optics, Siberian Branch of the Russian Academy of Sciences.
1, Academicheskii Av., Tomsk, 634055, Russia

8.PERFORMING ORGANIZATION REPORT NUMBER
N 199

9. SPONSORING MONITORING AGENCY NAME(S) AND ADDRES(ES)
U.S. Naval Regional Contracting Center Detachment London DoE Complex, Block 2, Wing 11, Eastcote Road RuiSlip, MIDDX, UK, HA 4 8BS

10. SPONSORING, MONITORING AGENCY REPORT NUMBER

11. SUPPLEMENTARY NOTES

12a. DISTRIBUTION/AVAILABILITY STATEMENT
Approved for public release; distribution unlimited

12b. DISTRIBUTION CODE

13. ABSTRACT (Maximum 200 words)

An effect of the atmospheric channel on near-ground propagation of acoustic waves is considered. The structure of the amplitude and phase fluctuations of acoustic waves propagating through the turbulent atmosphere near the ground has been analyzed. The structure of the temperature and wind velocity field and vertical profiles of the outer scale of atmospheric turbulence have been experimentally investigated.

14. SUBJECT TERMS Atmosphere, turbulence, temperature fluctuations, amplitude, phase, boundary layer, spektra, wind velocity

15. NUMBER OF PAGES 42

16. PRICE CODE

17. SECURITY CLASSIFICATION OF REPORT	18. SECURITY CLASSIFICATION OF THIS PAGE	19. SECURITY CLASSIFICATION OF ABSTRACT	20. LIMITATION OF ABSTRACT
Unclassified	Unclassified	Unclassified	UL

NSN 7540-01-280-5500

Standard form 298 (Rev 2-89)

ABSTRACT

An effect of the atmospheric channel on near-ground propagation of acoustic waves is considered. The structure of the amplitude and phase fluctuations of acoustic waves propagating through the turbulent atmosphere near the ground has been analyzed. The structure of the temperature and wind velocity fields and vertical profiles of the outer scale of atmospheric turbulence have been experimentally investigated.

LIST OF KEYWORDS

Atmosphere, turbulence, temperature, wind velocity, boundary layer, amplitude, phase, fluctuations, spektra

CONTENTS

1. INTRODUCTION

Investigations into the structure of the atmospheric boundary layer and acoustic waves propagating in it are very urgent and interrelated problems. The near-ground sound propagation has its peculiarities and differs from the sound propagation in free space. In addition to the meteorological parameters (the air temperature, the atmospheric pressure, the air humidity, and the wind speed and direction), geometric factors, for example, mutual arrangement of a source, a receiver, and an underlying surface also affect the near-ground sound propagation. In some cases, these factors may dominate in comparison with the effect of the meteorological parameters and hence call for much attention. In the present project, the above-indicated problems have been studied both theoretically and experimentally. The results of investigations were presented in 7 interim reports on this projects. This final report presents the results of our investigations into the effect of the atmospheric channel on the acoustic wave propagation above the ground as well as of investigations into the amplitude and phase fluctuations of acoustic waves propagating through the turbulent atmosphere near the ground and the structure of the temperature and wind velocity fields and the vertical profiles of the outer scale of atmospheric turbulence.

2. INFLUENCE OF THE ATMOSPHERIC CHANNEL ON THE SOUND PROPAGATION ABOVE THE GROUND SURFACE

It is well known that the atmospheric sound recorded from a stationary source essentially depends on meteorological conditions. This is caused by the high sensitivity of the total energetic losses of sound to such meteorological parameters as wind, temperature, relative air humidity, and atmospheric pressure. Mean values of humidity, temperature, and pressure determine not only the coefficient of molecular absorption of the acoustic radiation at a fixed frequency, but also its frequency dependence (Brown E.H. and Hall F.F., 1978; Harris C.M., 1966). Fluctuations of acoustic refractive index, caused by turbulent pulsations of the meteorological parameters, affect an interference pattern of directly transmitted and reflected acoustic rays and cause the excess turbulent attenuation (Brown E.H. and Hall F.F., 1978; Ingard U., 1953). In case of near-ground sound propagation at distances more than 1 km, sound attenuation is primarily affected by refraction on gradients of temperature and wind (Ostashev V.E., 1992), resulting in the waveguide or nonwaveguide regime of sound propagation. In the first case, rays bend downward and hence undergo multiple reflections from the ground. Relatively small values of sound attenuation are typical of this regime of sound propagation. In the second case, rays bend upward, and a shadow zone is formed near the ground at certain distances from the source. Only very weak sound, caused by turbulent scattering in the upper atmospheric layers, penetrates into this zone.

Previously we described the application package Outdoor Acoustics (Abramov N.G. et al., 1994; Bogushevich A.Ya. and Krasnenko N.P., 1993, 1996) for calculation of the sound pressure level in case of sound propagation through the atmosphere in the waveguide or nonwaveguide regime at distances up to 10 km and reported the field measurements that confirmed reliability and accuracy of the calculated data. In the present work, an attempt is made to analyze numerically, with the use of this application package, the effect of the meteorological parameters on audibility of sound in the atmosphere. The most interesting results of calculations are shown in Figures 1-4.

The dependence of the total attenuation L on the wind component parallel to the direction of sound propagation V_p is shown in Fig. 1. Here, the waveguide regime of propagation is realized for $V_p>0$ and the nonwaveguide regime - for $V_p<0$. Refraction by wind velocity gradients always results in the increase of sound attenuation. In the waveguide regime of propagation, the increase of V_p is accompanied by a relatively small increase in $|L|$, as a rule, by no more than 6-10 dB, connected with the change of the beam focusing pattern compared with the conventional spherical beam divergence. At the same time, in the nonwaveguide regime of propagation, the excess sound attenuation due to wind is much greater and may even exceed 100 dB. In this case, the sharp increase of $|L|$ by 15-20 dB is first observed as $|V_p|$ increases and the observation point enters the acoustic shadow zone. With the further increase of $|V_p|$, the sound attenuation continues to increase noticeably, because the atmospheric layer, from which a scattered signal comes to the observation point, is displaced upward. The change of the distance from the source d affects insignificantly the form of the dependence $L(V_p)$, but shifts noticeably the absolute values of L.

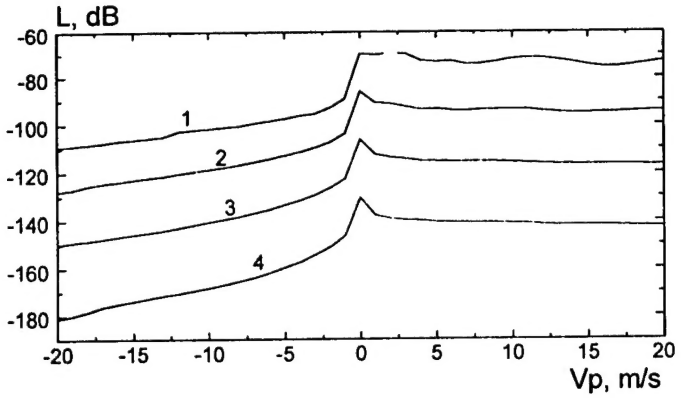

Fig. 1. The dependence of sound attenuation in the atmosphere, in dB, on the wind component V_p parallel to the direction of sound propagation for P=750 mm Hg, U=75%, T=20°C, γ=0°/km, $C_n^2=10^{-6}$ $m^{-2/3}$, f=1000 Hz, and distances to the source d=1(1), 3(2), 6(3), and 10 km(4).

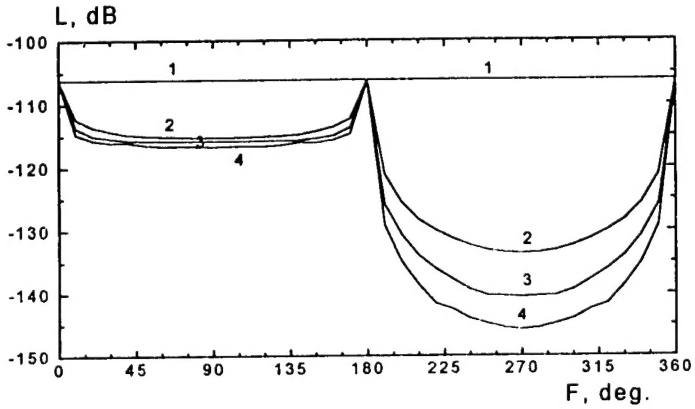

Fig. 2. Sound attenuation in the atmosphere, in dB, as a function of the wind direction F for U=75%, T=20°C, g=0°/km, $C_n^2=10^{-6}$ $m^{-2/3}$, f=1000 Hz, and V=$|\mathbf{V}|$ =0 (1), 5 (2), 10 (3), and 15 m/s (4).

Figure 2 shows sound audibility as a function of the wind direction *F* counted off from the source-observer direction. Curve *1* was calculated without refraction (*V*=0). It can be easily seen that at *V=const* the change of *F* is equivalent to the change of the wind component V_p parallel to the direction of sound propagation. Therefore, curves *2*, *3*, and *4* exhibit practically the same behavior as in Fig. 1. From Fig. 2 it follows that the wind component perpendicular to the direction of sound propagation affects insignificantly its audibility.

Figure 3 shows the dependence of *L* on V_p for indicated values of the structure parameter of refractive index fluctuations C_n^2 that characterize the intensity of the atmospheric turbulence. As expected, C_n^2 affects most strongly the sound pressure level in the nonwaveguide regime of sound propagation. In this case, the recorded pressure level is almost proportional to C_n^2. Because C_n^2 varies over a wide range, sound audibility also undergoes large variations. In our case experimental values changed from 2 to 5 km.

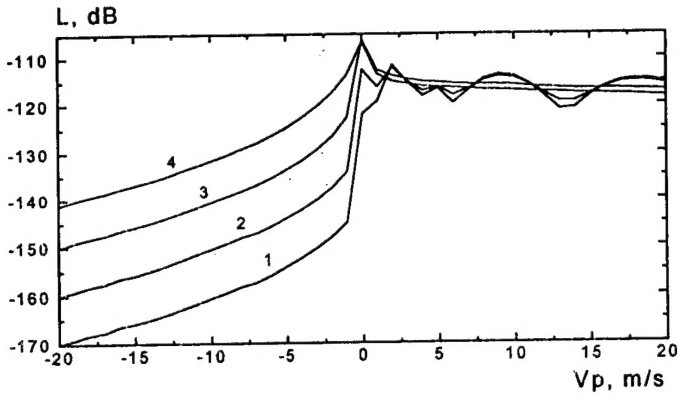

Fig. 3. Sound attenuation in the atmosphere, in dB, as a function of the wind component V_p parallel to the direction of sound propagation for U=75%, T=20°C, g=0°/km, f=1000 Hz, d=6 km, and $C_n^2=10^{-8}$ (1), 10^{-7} (2), 10^{-6} (3), and 10^{-5} $m^{-2/3}$ (4).

In the waveguige regime of propagation, the observed sound pressure level is a sum of pressure levels of individual rays propagating along paths of different lengths. The total pressure level differs qualitatively as a function of amplitude and phase fluctuations of rays. For small values of C_n^2, the amplitude and phase fluctuations of rays are also small and hence can be partly coherent. In this case, because the ray path lengths depend on the *V* profile, the linear increase of V_p results in the interference sound pressure pattern vividly seen in Fig. 3 for curves *1* and 2. For large values of C_n^2, the rays are incoherent and interference is not observed. Coherence starts to break at smaller values of C_n^2 as the distance between the source and the receiver increases.

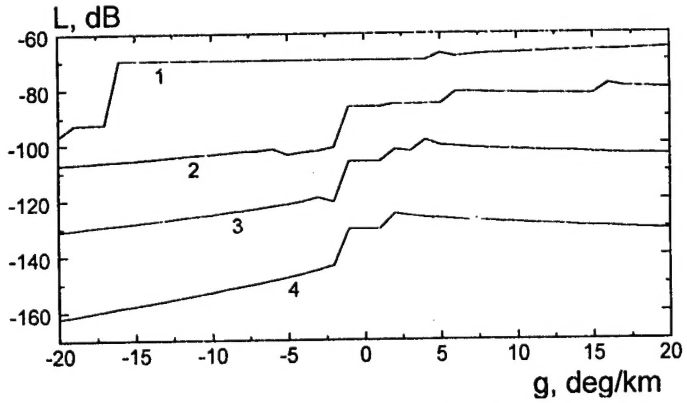

Fig. 4. Sound attenuation in the atmosphere, in dB, as a function of the temperature gradient g for U=75%, T=20°C, $C_n^2=10^{-6}$ $m^{-2/3}$, f=1000 Hz, and d=1 (1), 3 (2), 6 (3), and 10 km (4).

The effect of temperature gradient on sound attenuation in the atmosphere is illustrated by Fig. 4. For g>0, the waveguide regime of sound propagation is realized, as in the case of wind refraction for V_p>0, but in contrast to it, additional beam focusing takes place resulting in sound amplification. Therefore, the presence of temperature inversion in the atmosphere increases the sound level. In calculations, the sound source was at the distance r_1= 5 m above the ground and the observation point was at r_2=1.5 m. In the nonwaveguide regime of sound propagation, the zone of direct sound propagation always exists in the vicinity of the source followed by the acoustic shadow zone. For hight source and receive the distance to this shadow zone is determined by the curvature radii of ray paths, which are noticeably smaller in case of refraction by temperature gradients than in case of refraction by wind gradients. Therefore, when g <0 and the observation point is in the shadow zone, the sharp increase of sound attenuation takes place for large absolute values of g. The further increase of the sound attenuation in the shadow zone as |g| increases is caused by the upward displacement of the lower boundary of the region of sound scattering, as in the case of wind refraction.

3. ANISOTROPY OF THE AMPLITUDE FLUCTUATIONS OF THE ACOUSTIC WAVES PROPAGATED THROUGH THE TURBULENT ATMOSPHERE NEAR GROUND

The amplitude fluctuations of an acoustic wave, propagating in the ground layer of the turbulent atmosphere under conditions of reflection from the Earth's surface, were studied theoretically (Diaagle C.A., 1980; Clifford S.F., Lataitis R.L., 1983; Hidaka T., Kageyama K., Masuda S., 1985) and experimentally (Parkin P.H., Scholes W.E., 1965; Daigle G.A., Piercy J.E., Embleton T.F.W., 1978; Bochkarev N.N., Krasnenko N.P., 1986). In theory the peculiarities of an acoustic wave propagation in a randomly inhomogeneous moving medium (Ostachev V.E. 1992) were not taken into account while experimental investigations were conducted, as a rule, at a fixed path orientation relative to the wind velocity vector. In the experiment conducted we have developed and refined investigations, described in (Patrushev G.Ya., Postov A.P., 1996).

The difference of the results presented in this report from those published in (Patrushev G.Ya., Postov A.P., 1996) is as follows. We used more precise equipment. In the experiment, described in (Patrushev G.Ya., Postov A.P., 1996), for different directions different types of microphones and loudspeakers were used. There was also used an analog detecting of signals, with their following smoothing by low-frequency analog filters of the second order with further discretization at a frequency of 100 Hz. This could introduce additional error in the estimation of spatial anisotropy of the acoustic wave propagation. In this study we have used quite identical measuring condenser microphones and dynamic speakers. A 2-channel 12-bit high-speed ADCs (conversion time was 3 ms) were used for digitizing signals and correspondingly very high frequency of discretization of the signals themselves from the microphones. Also we used practically new method of the amplitude separation. The fast computer enabled using the programs working in real time and giving more exact results. All this allowed us to reach the identity of the through channels (emitter-microphone-recording accurate to 1% in the operating frequency band).

The approach to experimental data processing using low-frequency filtration with the following decimation (without smoothing) is quite different than that used in (Patrushev G.Ya., Postov A.P., 1996) and it allowed more exact study of the low-frequency portion of the spectrum.

In contrast to the study presented in (Patrushev G.Ya., Postov A.P., 1996) we arranged full meteorological measurements.

We analyzed the data acquired at different wind-temperature stratification, whereas in (Patrushev G.Ya., Postov A.P., 1996), the data obtained only at one (unstable) stratification were available. The synchronous measurements we have conducted of the relative amplitude fluctuations of an acoustic wave show significant anisotropy of fluctuations, depending on the average wind velocity, other conditions being the same. The diagram of the experiment is shown in Fig. 5.

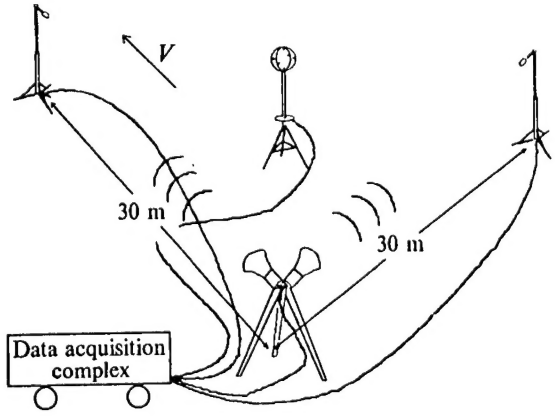

FIG. 5. Block-diagram of the experiment.

Two quasi-spherical waves directed along the average wind velocity and perpendicularly to it were measured simultaneously. Receiving microphones were at $L = 30$ m from the emitting horns. Emitters and receivers were located at the height $h = 1.5$ m. The loudspeaking horns with an output of 50 W used as the emitters, and as the receivers were used measuring condenser microphones MV201 by RFT, with the antiwind protection shields. Each microphone was connected to an ac pre-amplifier. The width of the receiver's directional pattern was close to 60°, and receiving microphones have the directional pattern of the cardioid shape. Signals from the amplifiers of the microphones entered the third-octave filters with the central frequency at 1.25 kHz. The output signals from the filters were digitized with a 12-bit ADC at a sampling frequency of 160 kHz and after the amplitude detection their values were entered in the computer memory at a frequency of 100 Hz. The amplitude detection was organized programmly using the following algorithm: 1600 digital values of the ADC codes were memorized in a buffer, then they were detected and the maximum value which was recorded as the instantaneous value of the amplitude was found from the obtained data array. This algorithm was realized on the assembler using the register addressation, thus enabling its real time operation.

Instantaneous values of the wind and temperature components were measured with a three-component ultrasonic anemometer-thermometer located at the height of $h = 1.5$ m at the bisectrix of the angle between the microphones. The flat field of flattened oats 15–20 cm high was the underlying surface. The frequency of the emitted wave was $f = 1.25$ kHz. Measurements were conducted both at stable and unstable stratification of the atmosphere and the time of an individual sampling was 300 s. The range of variation of the average temperature during the measurements at the height of $h = 1.5$ m was 1.5–6.8°, relative humidity of the air 99–75%, and the pressure 752–755 mm of the mercury column.

Further statistical processing of the obtained time series of the instantaneous values of the amplitude included the removal of rough errors using Chebyshev inequality, low-frequency filtration using Butterwort filter of the 6th order (Otnes R., Enokson L. 1982) and agreed with it decimation of the data with the index 8. Then the removal of the trend was conducted and autospectra were calculated after the FFT processing. The effect of infiltration was removed by the GEO window (Otnes R., Enokson L. 1982) after the calculation of the Fourier coefficient. In parallel with the autospectra the average values of the amplitudes, their variances and autocorrelation functions were also calculated.

$$\beta^2 = \frac{(\Lambda^2) - (\Lambda)^2}{(\Lambda)^2} = \frac{(\Lambda^2)}{(\Lambda)^2}$$

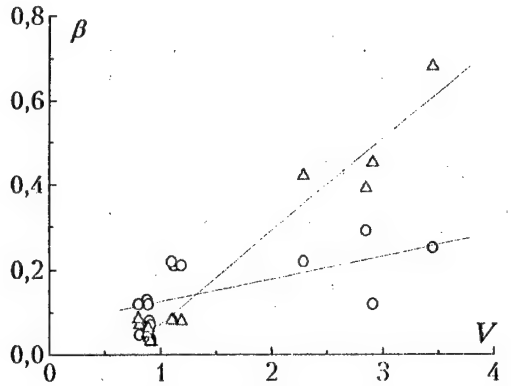

FIG. 6. The dependence of the relative rms deviation β on the average wind velocity V for the paths along (o) and across (Δ) the wind.

In Fig. 6 are shown the values of the relative rms deviation β of the amplitude fluctuations A, depending on the value of the average wind velocity V for longitudinal and transverse relative to the wind direction paths. The straight lines, constructed as the best linear approximation of the experimental data are also shown in the figure. As the obtained data show much stronger

dependence of the amplitude fluctuations on the wind speed is observed for the cross wind path as compared to that for the path along the wind.

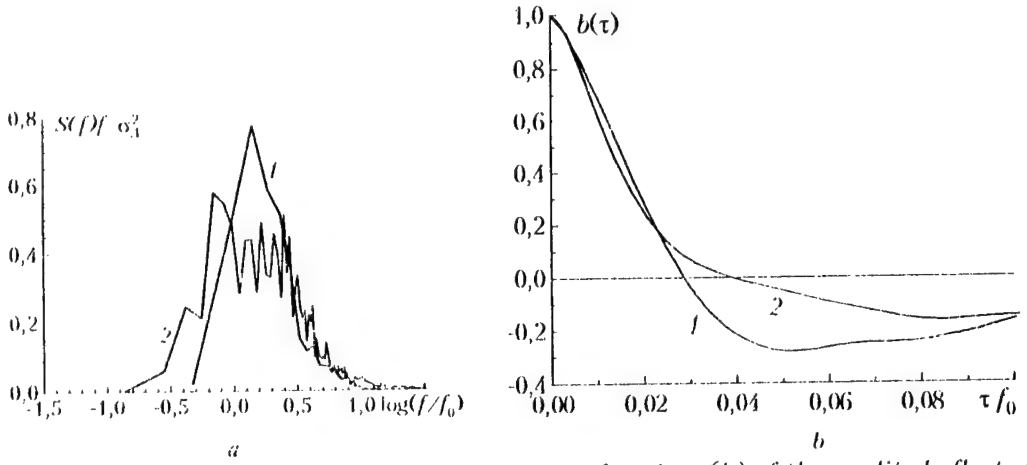

FIG. 7. The temporal spectra (a) and autocorrelation functions (b) of the amplitude fluctuations of an acoustic wave for the paths along (1) and across (2) the wind at a stable stratification of the atmosphere (ξ = +0.1): *1* – $V_\perp$ = 0.008 m/s; $\sigma_\perp$ = 0.3 m/s; *2* – $V_\perp$ = 0.9 m/s; $\sigma_\perp$ = 0.4 m/s.

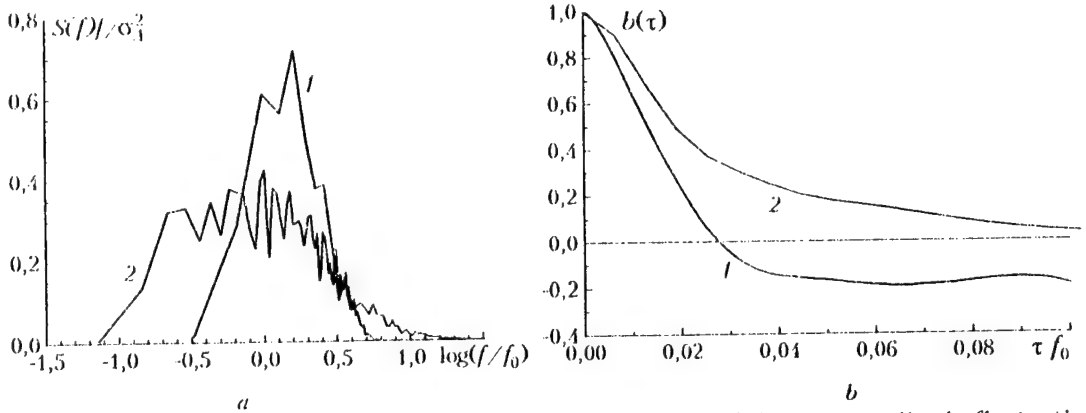

FIG. 8. The temporal spectra (a) and autocorrelation functions (b) of the amplitude fluctuations of an acoustic wave for the paths along (1) and across (2) the wind at an unstable stratification of the atmosphere (ξ = –0.9): *1* – $V_\perp$ = 0.06 m/s; $\sigma_\perp$ = 0.27 m/s; *2* – $V_\perp$ = 1.2 m/s; $\sigma_\perp$ = 0.32 m/s.

In Figs. 7 and 8 are shown the dimensionless temporal spectra of the amplitude fluctuations for both paths and corresponding to this spectra normalized temporal autocorrelation functions obtained at stable (Fig. 7) and unstable (Fig. 8) stratifications of the atmosphere. The scale of similarity considering variations of the average, perpendicular to the wind velocity $V_\perp$, and fluctuational component $\sigma_\perp$, is the characteristic frequency $f_0 = [(V_\perp^2 + \sigma_\perp^2)/(\lambda L)]^{1/2}$ (Patrushev G.Ya., Postov A.P., 1994), where λ is the length of the wave of radiation, L is the length of the path. From the data presented one can see that the time spectrum for the path perpendicular to the average wind undergoes broadening to the low-frequency region as compared to the time spectrum obtained for the path, directed along the average velocity of the wind, and moreover, under unstable stratification the broadening is considerably more noticeable and forms approximately half an order of magnitude on the scale of the relative frequences.

4. PHASE FLUCTUATIONS OF THE ACOUSTIC WAVE PROPAGATING NEAR GROUND

Fluctuations of phase difference of acoustic waves propagating in the turbulent atmosphere were theoretically studied in detail in (Tatarskii V. I., 1961, Chernov L.A., 1975), where their linear dependence on the structural characteristic of the refractive index fluctuations C_n^2 and on the length of the propagation path L and $k^{7/6}$ dependence on the wave number were established. The temporal spectrum of phase difference fluctuations depends on the length of measurement path and the average wind velocity component perpendicular to the propagation path. The form of the probability density of phase difference fluctuations $P(\phi)$ was not discussed; however, in the geometric acoustics approximation and in the context of the smooth perturbation method the Gaussian probability density of phase difference fluctuations should be expected when the central limit theorem is applicable. Up to now, the problem of saturation of phase fluctuations under different propagation conditions also was not discussed.

Experiments performed under conditions when the effect of the ground can be neglected agree fairly well with the theory based on the method of geometric acoustics for the Kolmogorov spectrum of atmospheric turbulence. Experimental data on the phase difference fluctuations σ_ϕ^2 and on the fluctuations of the mutual coherence function were reported in (Daigle G.A. et al., 1983). The measurements there were carried out for propagation paths of lengths L from 2 to 300 m and were accompanied by independent measurements of the atmospheric meteorological parameters. Two transient phase meters were used to measure the phase difference. They were capable of measuring phase differences up to 2π rad and were shifted by π rad. It should be noted that operation of the phase meters was controlled by a computer, which assigned the constant phase difference to those readings of the phase meter for which the input signal died down and was less than the threshold specified by the operating instructions to these phase meters. Obviously, this can be considered as a disadvantage, because the signal phase undergoes fast variations exactly when the input signal dies down. These fast phase variations cannot be measured by this method. Nevertheless, Daigle et al., 1983 obtained good agreement between their experimental data and calculations for the Gaussian spectrum of atmospheric turbulence with the finite value of the outer scale of turbulence L_0. It should be mentioned that the measurements were carried out above asphalt-coated underlying surface, and the receiver was located outside the refraction shadow zone. To this end, the receiver height above the ground was changed with the increase of the measurement path length. The increase of the receiver height should cause the increase of the outer scale of atmospheric turbulence; however, for their calculations Daigle et al., 1983 used constant value of the outer scale of turbulence L_0=1.1 m even for the receiver height as great as 7 m. Other characteristics of the acoustic wave phase fluctuations were not considered in that paper.

We measured the acoustic wave phase difference for propagation paths 50, 100, 200, and 400 m long. Receiving microphones were spaced at $d\cong$1 m. Their heights above the ground were h_1=1 m in the first series of measurements and h_2=0 in the second series of measurements, that is, the receivers were placed directly on the ground. A source was at heights h_s=(1.3–1.5) m above the ground. For this geometry of the experiment, the source can be considered as a source of spherical acoustic waves with a frequency of 1 kHz.

Figure 9 shows the rms values of the phase difference fluctuations σ_ϕ versus the parameter $\beta=0.308 C_n^2 L^{11/6}(2\pi f/V_s)^{7/6}$ that specifies the conditions of sound wave propagation in free space as functions of the structural characteristic of the refractive index fluctuations C_n^2, propagation path length L, and the acoustic wave number $k=2\pi f/V_s$. Here, V_s is the speed of sound. In the figure, circles are for the first series of measurements with h=1 m, and crosses are for the second series of measurements, when the receivers were placed on the ground. During our measurements we could not record signals simultaneously for different propagation path lengths L under the same meteorological conditions (determined by the structural characteristic of the refractive index fluctuations and gradients of the air temperature and wind velocity). Therefore, it was quite reasonable to choose the parameter β to characterize the conditions of acoustic wave propagation. It can be seen from the figure that the rms values of phase difference increase when the parameter β increases by about two orders of magnitude. On the semi-logarithmic scale, this dependence can be approximated by a straight line. However, some data recorded for small β disobey this dependence. It should be noted that for long propagation paths with L=400 m the experimental phase difference σ_ϕ was close to that reported in Daigle et al, 1983. We could not compare our data more accurately, because (Daigle et al, 1983) did not indicate the distance between the receivers. It also can be seen from the figure that the behavior of the phase difference is practically the same for the receivers located at two heights h=0 and 1 m.

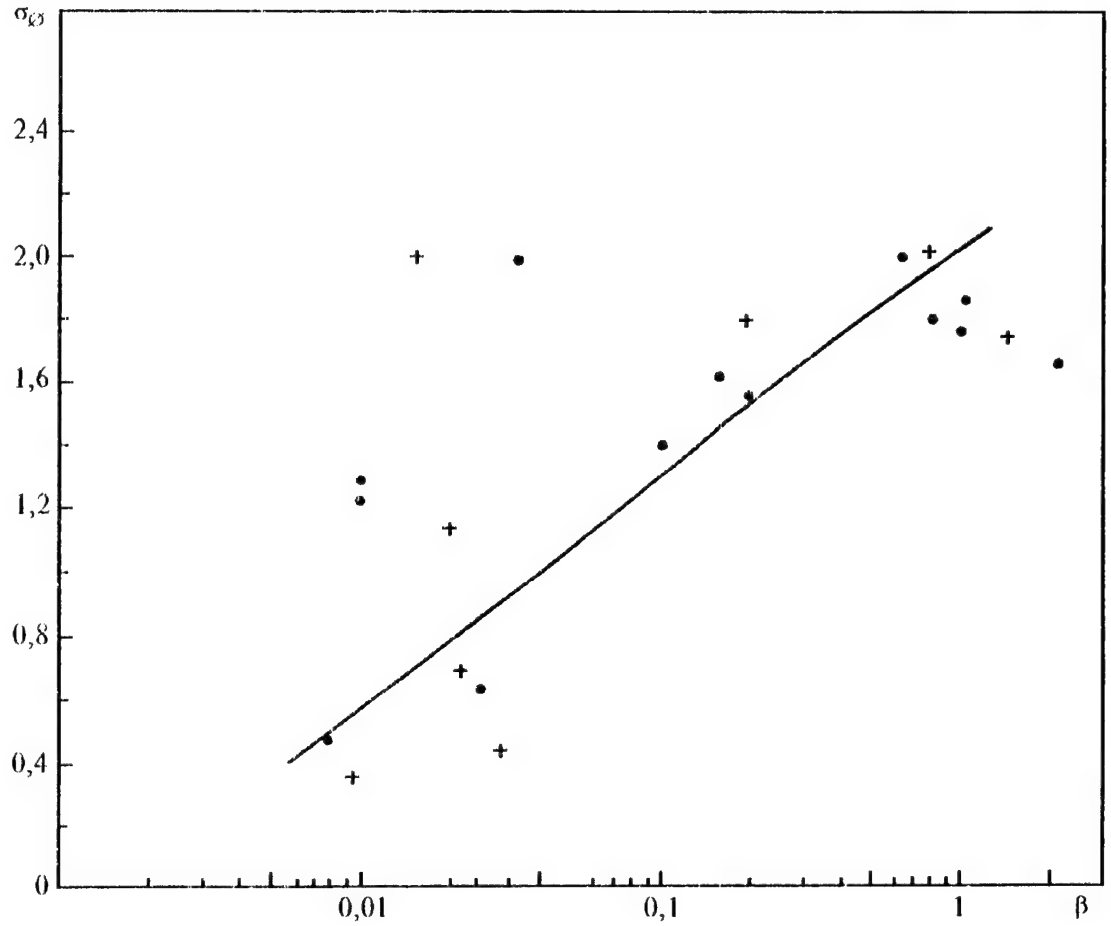

Fig. 9. Dependence of the magnitude of phase fluctuations on the parameter β

The probability density characterizes more adequately the fluctuations of a random variable. Up to now, as already mentioned above, no experimental data were reported for this characteristic (at least, they are unknown to us). This characteristic also was not investigated theoretically. At the same time, our experimental procedure can be used to study the probability density of the phase difference $P(\phi)$. Curve 1 in Fig. 10 shows the histogram of the phase difference $P(\phi)$ for the propagation path of length L=100 m, height of the receivers h=1 m, σ_{ϕ}=0.44, and β=0.037. Curve 2 shows the Gaussian probability density drawn for the same variance. It can be seen from the figure that the distribution of the measured fluctuations of the acoustic wave phase difference significantly deviates from the normal distribution, namely, its modal value is more probable and large values of phase difference are less probable. Such behavior of the probability density was typical of practically all experimental histograms of phase difference fluctuations, not only for measurements with the receivers located directly on the ground, but also for measurements with the receivers placed at heights of 1 m above the ground and spaced in the horizontal direction.

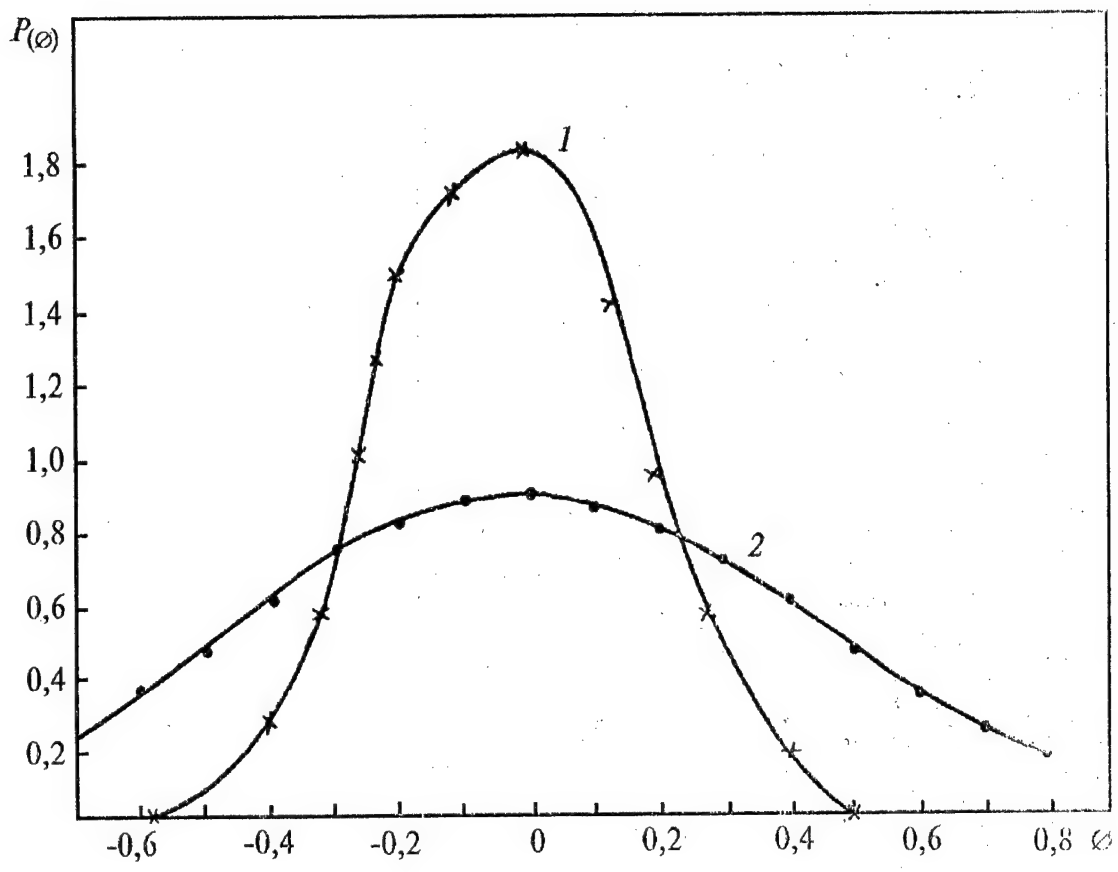

Fig. 10. Comparison of the experimental probability density $P(\phi)$ (curve *1*) with the normal probability density (curve *2*)

Figure 11 shows the temporal spectra of fluctuations of acoustic wave phase difference recorded with the receivers located at heights of 1 m above the ground under conditions of strongest wind velocity V=4 m/s measured at a height of 3 m above the ground (curve 2) and when the wind velocity measured at a height of 3 m was V=0.39 m/s (curve 1). The logarithm of the frequency f (in Hz) is plotted on the abscissa, and the spectral power density $G(f)$ normalized to the variance σ_ϕ^2 and multiplied by the frequency f is plotted on the ordinate. The dimensionless spectrum $U(f)=fG(f)/\sigma_\phi^2$ can be used to estimate the contribution of different frequencies to the fluctuation variance in a wide spectral range. As follows from the theory of acoustic wave propagation, the temporal spectrum of phase fluctuations broadens linearly with the increase of the wind velocity component orthogonal to the propagation path in the free atmosphere (the similarity parameter is $fd/V_\perp$). As can be seen from the figure, a 10-fold increase of the wind velocity component perpendicular to the propagation path caused the shift of the position of the spectral power density maximum toward larger frequencies. Its frequency increased no more than twice. That is, the dependence of the temporal spectrum of the phase difference fluctuations on the perpendicular component of the wind velocity is very weak in case of near-ground propagation. It also should be noted that the characteristic fluctuation frequencies were no more than 20-30 Hz, and the maximum of the dimensionless spectrum was about 0.3, which was typical of the propagation in the free atmosphere. An analysis of the temporal phase difference spectra showed that they did not depend on the propagation path length and the intensity of atmospheric turbulence for the considered heights of receivers (h=0 and 1 m) when all other factors remained unchanged.

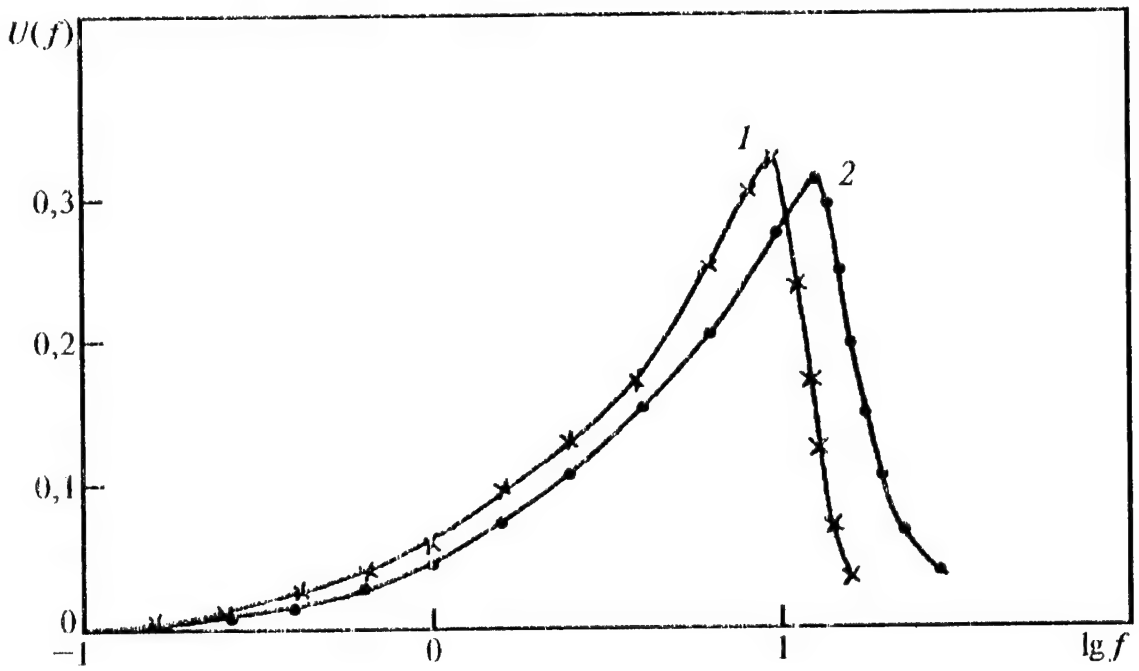

Fig. 11. Temporal spectra of fluctuations of phase difference for 1-m separation of the receivers and V_1=0.39 (curve *1*) and 4 m/s (curve *2*)

To calculate the mutual coherence function, we used the discrete Hilbert transform. According to the definition, let $x_1(t)$ be the instantaneous value of the signal $x_1(t)=A_1(t)\exp[i(2\pi ft+\alpha_1(t))]$, where $A_1(t)$ and $\alpha_1(t)$ are real random functions, and analogously, $x_2(t)$ $A_2(t)\exp[i(2\pi ft+\alpha_2(t))]$. Then the mutual coherence function G_{12} can be written as

$$\Gamma_{12}=\frac{<\dot{A}_1(t)\,\dot{A}_2^*(t)>}{\left[<\dot{A}_1(t)\,\dot{A}_1^*(t)>\right]^{1/2}\left[<\dot{A}_2(t)\,\dot{A}_2^*(t)>\right]^{1/2}}$$

where the angular brackets denote time averaging defined by the formula

$$<\ldots>=\frac{1}{T}\int_0^T(\ldots)\,dt$$

Figure 12 shows the mutual coherence functions on the propagation path of length 50 m for the values of the parameter β=0.009-0.01 and for the propagation path of length 400 m and β=0.9-1.6. It can be seen that the degree of coherence decreases noticeably for longer propagation path. It also should be noted that the mutual coherence function measured in (Daigle et al, 1983) at a frequency of 1 kHz for the propagation path of length 100 m with the receivers spaced at a distance of 1 m was much greater. This may be explained by the fact that the receivers were placed at greater heights above the ground than in our measurements as well as by different type of the underlying surface (hard covering and cultivated field sowed with peas and oats).

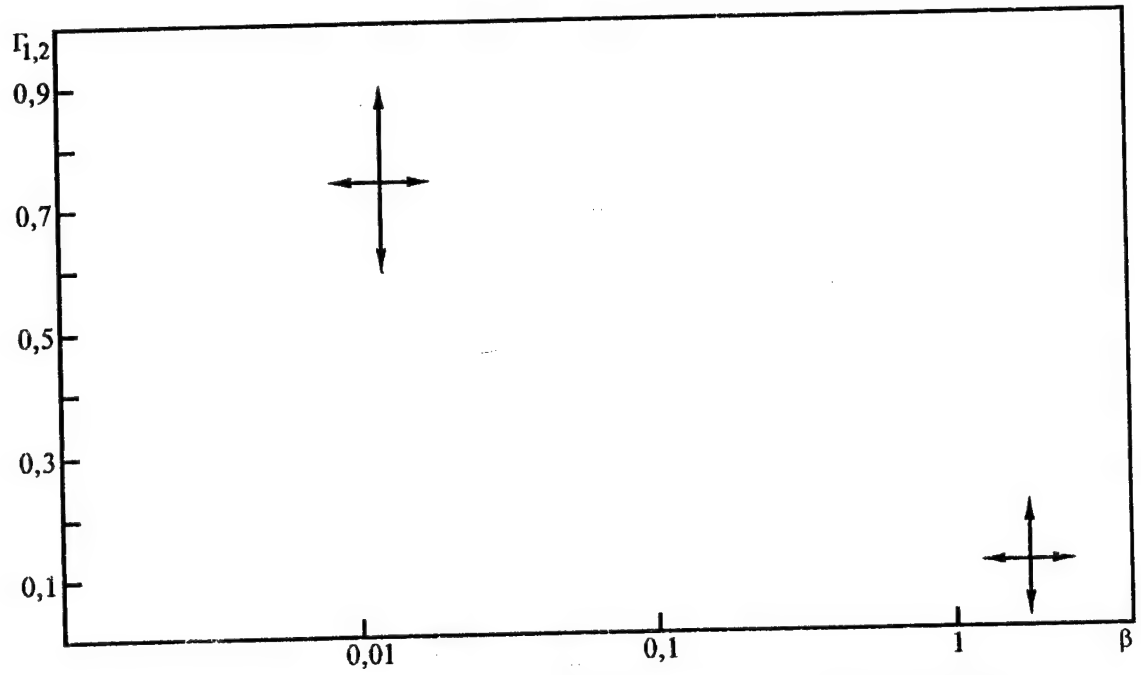

Fig. 12. Mutual coherence function Γ_{12} on the paths 50 ($\beta \approx 0.01$) and 400 m long (β=0.9-1.6)

To summarize the results of our investigations of statistical characteristics, we can conclude the following:

In summer the rms values of the intensity fluctuations of acoustic waves propagating near the ground varied by about an order of magnitude on paths of lengths from 50 to 400 m for the receivers spaced at 1 m as functions of the intensity of atmospheric turbulence.

The probability density of fluctuations of phase difference significantly deviated from the normal one. The temporal spectra of fluctuations depended on the wind velocity measured at the height of receiver location much weaker than in case of line-of-sight propagation. With the increase of the propagation path length the mutual coherence function measured at a frequency of 1 kHz decreased. For path 400 m long and receivers spaced at 1 m it was between 0-0.3.

Our measurement method is rather adaptable. It allowed us to study all statistics of phase fluctuations. To improve the method, we should improve the measurement procedure including synchronous recording of signals for several propagation paths and different separations of the receivers and measurements of the outer scale of atmospheric turbulence.

5. EXPERIMENTAL VERIFICATION OF A MODEL FOR THE SPECTRAL TENSOR OF THE WIND VELOCITY FIELD

Detailed structure of small-scale turbulence of lower layers of the atmosphere is interesting from different points of view. There is a wide scope of applied problems requiring adequate description of the spatial spectrum of turbulent pulsations of wind velocity in the surface layer. Information of such a kind is necessary, for instance, in the problems on propagation of optical and radio waves in the atmosphere, in solving problems of acoustic and lidar sounding, for taking account of pollutant dispersal in ecological problems, for estimation of spatial variability of wind pressure in calculating constructional stresses, etc.

According to modern experimental and theoretical data, the three-dimensional spatial spectrum of turbulent pulsations of wind velocity is a tensor of the second rank.

In the approximation of isotropic turbulence (Tatarskii V.I., 1961), the spectral tensor $\Phi_{ij}(\mathbf{k})$ is completely determined by a single scalar function of the wave number $k = |\mathbf{k}|$

$$\Phi_{ij}(\mathbf{k}) = (4\pi k^2)^{-1}\{\delta_{ij} - k_i\, k_j\, k^{-2}\}E(k)\ , \tag{5.1}$$

namely, by the energy spectrum $E(k)$ for which the Kolmogorov–Obukhov law of "five thirds": $E(k) \sim \varepsilon^{2/3}k^{-5/3}$, where ε is the dissipation rate of the turbulence kinetic energy, should hold for reasons of dimensionality.

The isotropic approximation in the surface layer sufficiently well works in the inertial interval of the wave number. However, the turbulence becomes anisotropic with the increase of spatial scales and approaching the energy interval of the spectrum (Newstadt F.T.M., Van Dop H., 1985). In fact, when the distance between the observation points of wind velocity fluctuations is comparable with the outer turbulence scale, the hypothesis on the spatial isotropy of fluctuations fails. So it is necessary to construct better models for the spectral tensor.

According to the Monin–Obukhov similarity theory, the dimensionless spectra of fluctuations of wind velocity vector components in the surface layer of the atmosphere at the height z are universal functions of the dimensionless wave number kz and the stratification parameter z/L, where L is the Obukhov scale. This means that specified characteristic frequencies corresponding to spectral maxima, low-frequency boundaries of the inertial interval, etc. depend on the stratification (Zilitinkevich S.S., 1970). Thus, the similarity theory permits one to make some concrete conclusions about the shape of the spectra under different states of the surface layer stability. Thus, the attempts to take into account some universal regularities in the surface layer by the similarity theory and experimental data are quite urgent in simulation of the spectral tensor.

The kinematic model of turbulence developed by Kristensen L., Lenshow D.H., Kirkegaard P., Courtney M., 1989 is of special interest among the investigations on this problem. It is based on the representation of the spatial spectrum of the velocity field fluctuations as an anisotropic tensor $\Phi_{ij}(\mathbf{k})$. The following form is proposed in the above-mentioned paper for the spectral tensor in the approximation of a homogeneous incompressible turbulent flow:

$$\Phi_{ij}(\mathbf{k}) = \sum_{l=1}^{3} A_l(k)\,\{\delta_{li} - k_l\, k_i\, k^{-2}\}\{\delta_{lj} - k_l\, k_j\, k^{-2}\}. \tag{5.2}$$

In contrast to the case of isotropic turbulence (5.1), the description of the tensor (5.2) needs three independent real scalar functions $A_1(k)$, $A_2(k)$, $A_3(k)$ determining the energy of turbulent vortices along three orthogonal directions assigned by unit vectors $\mathbf{i}_1$, $\mathbf{i}_2$, $\mathbf{i}_3$.

Variances σ_u^2, σ_v^2, σ_w^2, integral scales l_u, l_v, l_w, and dimensionless parameters μ_u, μ_v, μ_w characterizing the spectrum inclination in the transition range from the inertial interval to the

energy interval of wave numbers are used in (Kristensen L., Lenshow D.H., Kirkegaard P., Courtney M., 1989) as the parameters describing the behavior of the spectra of longitudinal, transverse, and vertical components u, v, w of the velocity. Here, the analytical expressions for one-dimensional spatial spectra of fluctuations of the velocity components have the form

$$F_u(k) = \frac{l_u \sigma_u^2}{\pi}\left\{1+\left(\frac{l_u k}{a(\mu_u)}\right)^{2\mu_u}\right\}^{-\frac{5}{6\mu_u}},$$

$$F_v(k) = \frac{l_v \sigma_v^2}{2\pi}\left\{1+\frac{8}{3}\left(\frac{l_v k}{a(\mu_v)}\right)^{2\mu_v}\right\}\left\{1+\left(\frac{l_v k}{a(\mu_v)}\right)^{2\mu_v}\right\}^{-\frac{5}{6\mu_v}-1}, \qquad (5.3)$$

where $a(\mu) = \{\pi\mu\Gamma[5/6\mu]\}/\{\Gamma(1/2\mu)\Gamma[(1/3\mu)]\}$ is a dimensionless constant determined by the normalization condition $\sigma^2 = \int_{-\infty}^{\infty} F(k)dk$ for each concrete value; k is the wave number along the direction of the mean horizontal velocity. The expression for $F_w(k)$ is similar to that for $F_v(k)$ given the corresponding change of indices.

Thus, one uses nine parameters as "input" information for constructing the model of tensor (5.2). The analytical dependences of A-functions on these parameters proposed in (Kristensen L., Lenshow D.H., Kirkegaard P., Courtney M., 1989) are not presented here because they are too cumbersome. In our opinion, an advantage of the approach considered is that the input parameters of the model can be obtained in two ways: first, by model assignment depending on the conditions of stratification and scaling on the basis of similarity theory (here, one can use data already published in order to reach more high level of generalization); second, by direct determination of the unknown parameters on the basis of approximation of the experimentally measured spectra by expressions (5.3) according to the least-squares method followed by calculation of A-functions and the tensor (5.2). The implied possibility of a model description of the spatial structure of homogeneous anisotropic turbulence with the exclusion of the necessity to perform measurements at many points is very attractive from the practical point of view. But the model considered has some shortcomings. In particular, it cannot guarantee positive definiteness of the tensor (5.2) for arbitrary input parameters.

The coherence function

$$\Gamma_{ij}^2(\mathbf{R}, \omega) = |W_{ij}(\mathbf{R}, \omega)|^2 / |W_{ij}(0, \omega)\, W_{ji}(0, \omega)|, \qquad (5.4)$$

where $W_{ij}(\mathbf{R}, \omega) = \frac{1}{2\pi}\int_{-\infty}^{\infty} B_{ij}(\mathbf{R}, \tau)\exp(-i\omega\tau)d\tau$ is the mutual spectrum of fluctuations at two spatially separated points, is one of the most informative characteristics among others being used to describe statistical laws of the spatial structure of the random wind velocity field.

Let the observation points be separated in a horizontal plane by the distance R normally to the mean wind direction. Using the hypothesis of frozen turbulence and expansion into the three-dimensional spatial spectrum for the spatiotemporal correlation function $B_{ij}(\mathbf{R}, \tau)$ and the model representation (5.2), one can obtain the following expressions[4] for the mutual spectra of longitudinal, transversal, and vertical velocity components:

$$W_{11}(R, \omega) = 2\pi v^{-1}\int_0^{\infty} k^3 \kappa^{-4}\{k^2 J_0(Rk)\, A_1(\kappa) + \omega^2 v^{-2}\,[J_0(Rk) - R^{-1} k^{-1} J_1(Rk)]A_2(\kappa) +$$

$$+ \omega^2 v^{-2} R^{-1} k^{-1} J_1(Rk) A_3(\kappa)\}dk;$$

$$W_{22}(R, \omega) = 2\pi v^{-1} \int_0^\infty k \kappa^{-4}\{ \omega^2 v^{-2} k^2[J_0(Rk) - R^{-1} k^{-1} J_1(Rk)]A_1(\kappa) + [(\omega^4 v^{-4} - 3R^{-2} k^2)J_0(Rk) +$$

$$+ 2R^{-1} k(\omega^2 v^{-2} + 3R^{-2})J_1(Rk)]A_2(\kappa) + R^{-2} k^2[3J_0(Rk) + (R^2 k^2 - 6)R^{-1} k^{-1} J_1(Rk)]A_3(\kappa)\}dk;$$

$$W_{33}(R, \omega)=2\pi v^{-1} \int_0^\infty k\kappa^{-4}\{\omega^2 v^{-2} R^{-1} k J_1(Rk)A_1(\kappa)+R^{-2}k^2[3J_0(Rk)+(R^2k^2-6)R^{-1}k^{-1}J_1(Rk)]A_2(\kappa)+$$

$$+[(\kappa^4 - 3 R^{-2} k^2)J_0(Rk) - 2(\kappa^2 k^2 - 3 R^{-2} k^2) R^{-1} k^{-1} J_1(Rk)] A_3(\kappa)\}dk, \qquad (5.5)$$

where $k = \sqrt{k^2 + \omega^2 v^{-2}}$; $J_n(x)$ are Bessel functions of the nth order.

Thus we can calculate coherence, i.e., obtain information about the spatial structure of an anisotropic wind velocity field as a whole within the frames of the homogeneous turbulence approximation by using the parameters of velocity component autocorrelation spectra measured experimentally at a single point as an input information.

Since most of the investigations are restricted by the use of isotropic turbulence approximation, experimental measurements of coherence are not enough complete to perform detailed comparison with the model prediction.

The aim of the study presented in this report is to experimentally verify the spectral tensor model of Kristensen L.et al., 1989 which is not isotropic but includes isotropy as a particular case.

The acoustic weather station, which is a compact program-simulated device and enables one to obtain data about each component of the wind velocity, temperature, and their fluctuations at frequency up to 20 Hz and to measure air pressure and humidity, was the principal measuring instrument in the experiments performed. Two to three such weather complexes controlled by a personal computer were used in the experiments, and this made it possible to realize long-term automated measurements and data storage. Different spatial arrangements of the weather stations both in the horizontal and a vertical planes were used in different experiments. The processing of measurement data included the calculation of autocorrelation spectra and coherence spectra for all the three velocity components, friction rate, temperature scale, flows of momentum and heat, Obukhov scale, and Richardson's number what made it possible to monitor the state of the surface layer by stratification conditions. Some preliminary results of the investigations are published in the 1st interim report.

In general, the investigations performed confirm the existence of strong anisotropy of the wind velocity field fluctuations in the surface layer and the dependence of the pulsation energy distribution over the space of wave numbers on the shape of the corresponding one-dimensional spectra $F_u(k)$, $F_v(k)$, $F_w(k)$. At the same time, the A-functions calculated in accordance with the model prove to be negative in the region of small wave numbers in some cases for particular parameters of the spectra σ^2, l, μ obtained experimentally. This leads to the break of the positive definiteness condition of the tensor $\Phi_{ij}(\mathbf{k})$, and we obtain coherence greater than unity for the corresponding velocity component.

This discrepancy is caused by the drawbacks of the model related to the fact that, in real experiments, one often observes nonstationarity caused by daily radiation fluctuations and leading to change of the heat flow H depending on time and height. This effect is especially strong under the spacing R considerably exceeding the value of the outer turbulence scale. However, the contribution of negative values of A_3 corresponding to large-size vortices decreases for horizontal spacing equal or somewhat less than l_u, and the model coherence does not exceed unity.

The spectra of wind velocity components measured over the plain underlying surface at midday time in summer under unstable stratification of the surface layer for $z/L = -0.064$ and normalized by the variance are presented, as an example, in Fig. 13. The sample contains 8192 synchronously measured values of three wind velocity components and temperature. The measurements were performed at a rate of 10 Hz during 13.65 min.

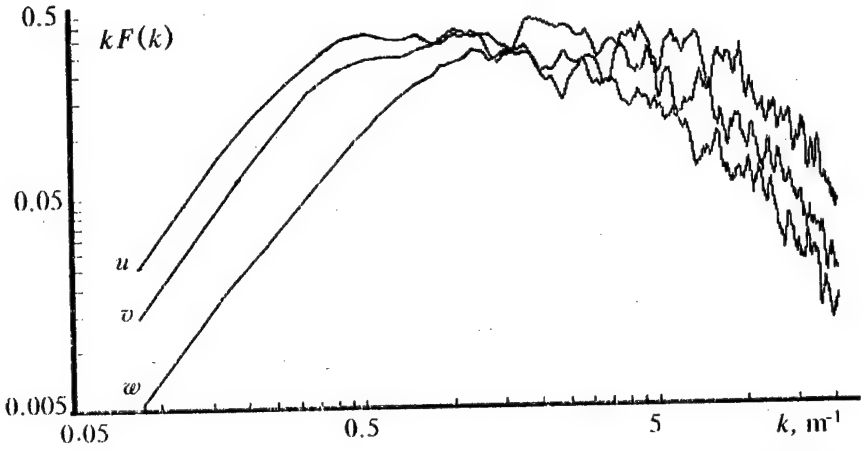

FIG. 13. One-dimensional spectra for the longitudinal, transverse, and vertical wind velocity components, u, v, w, obtained experimentally.

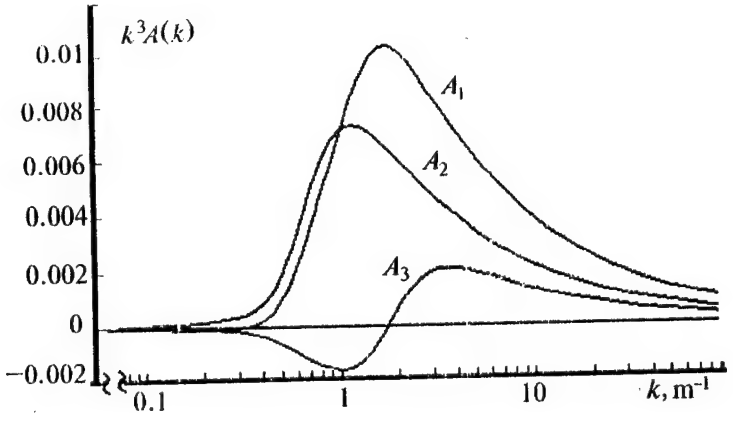

FIG. 14. Three model A-functions determining the spectral tensor, calculated for the spectra depicted in Fig. 13.

The whole sample was divided into 16 sequential intervals containing 512 points each in order to increase the degree of freedom in the spectral processing. Linear filtration of data was carried out using the approximation with a polynomial of the first degree followed by subtraction from the initial data array. So the trend effects in the wind velocity were excluded. The spectra calculated for each interval were summed up and normalized by the sample variance. The resulted spectra were smoothed over five neighboring points. According to our estimations, the relative error of the spectrum estimation using this processing does not exceed 11%. The values of wind velocity

components averaged over measurement time were as follows: $V_u = 1.446$ m/s, $V_v = 0.000$ m/s, $V_w = -0.086$ m/s. Spectral parameters obtained by the least-squares method for these velocities are equal to

$\sigma_u^2 = 0.190$ m^2/s^2	$\sigma_v^2 = 0.145$ m^2/s^2	$\sigma_w^2 = 0.056$ m^2/s^2
$l_u = 1.074$ m	$l_v = 1.095$ m	$l_w = 0.426$ m
$\mu_u = 1.2$	$\mu_v = 1.5$	$\mu_w = 1.61$

Figure 14 presents three Λ-functions determining the spectral tensor (5.2) and calculated for the above-mentioned parameters in correspondence with the model of Kristensen L.et al., 1989. Figure 15 presents the coherence spectra calculated by formulas (5.4) and (5.5), and those obtained experimentally at the transverse horizontal separation $R = 0.5$ m. A little excess of the experimental coherence over the calculated one can be explained, on the one hand, by the shortcomings of the model restricted by the hypotheses of frozen and homogeneous turbulence and, on the other hand, by errors in determining input parameters of the model and in performing the model calculations. Since the model considered imposes increased requirements on the correctness of statistical processing of the measurement data, it is necessary to eliminate low-frequency trends in the initial temporal series of data in order to increase the reliability of spectral estimations in the region of low frequencies.

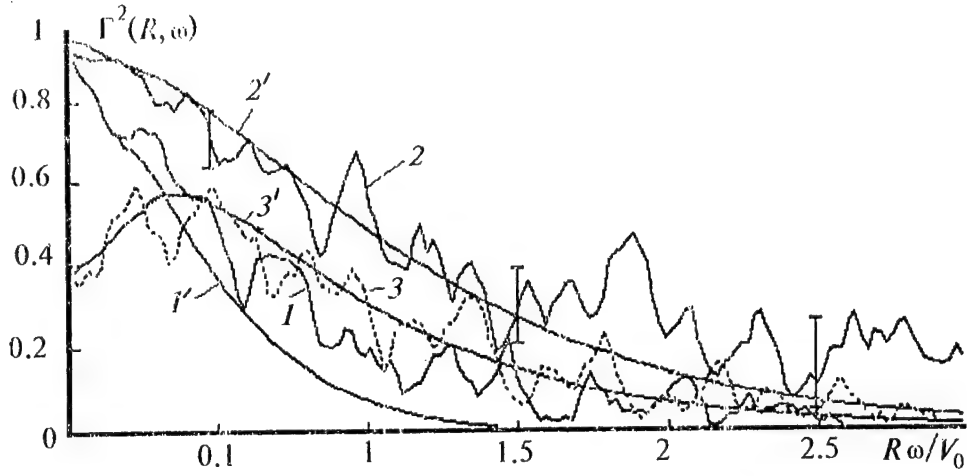

FIG. 15. Coherence spectra for longitudinal (1, 1'), transverse (2, 2'), and vertical (3, 3') wind velocity components obtained experimentally (curves 1–3) and calculated by the model (1'–3').

On the basis of a good coincidence of the predicted and the experimentally measured coherence, one can come to a conclusion that the model considered can be useful in estimating spatial statistics of turbulent pulsations using information obtained at a single point of the space when the conditions of the experiment correspond to the accepted hypotheses.

6. STUDY OF STATISTICAL PROPERTIES OF THE WIND AND TEMPERATURE FIELDS IN THE ATMOSPHERIC SURFACE LAYER WITH ULTRASONIC SENSORS

At present to develop and substantiate theoretically the lidar and acoustic methods of sounding the atmospheric parameters normally the Kolmogorov model of turbulence for locally isotropic medium is used. In this case a spatiotemporal structure of wind velocity field is described using the hypothesis of "frozen" turbulence, and temperature is considered as a conservative and passive impurity. But, as known, in the atmospheric surface layer the turbulence is essentially anisotropic. Moreover, there are differences in the behavior of the wind and temperature fluctuations depending on the stability state of the atmosphere (Newstad F.T.M. and Van Dop H., 1985)

In this report we consider some results of a series of experiments to study in detail the structure of turbulence in the atmospheric surface layer using six ultrasonic sensors of wind velocity and temperature fluctuations. The primary goal of the study was to elucidate a dependence of statistical characteristics of fluctuations of the wind velocity and temperature on a variety of parameters: the distance between the measurement points, direction of separation with respect to average velocity, frequency, and thermal stratification conditions in the surface layer.

Measurements were carried out during twenty four hours every half an hour. Spatially the ultrasonic sensors were placed along one line at a distance of 1 m between them. Measurements of fluctuations of the longitudinal wind velocity component and temperature were made with all the six sensors. Moreover, the acoustic weather station (Rostov A.P., 1993), which measured the fluctuations of three wind velocity components, temperature, humidity, and average value of air pressure, was used as one of the sensors. The measurements were made synchronously at a rate of 4 Hz. The length of a single data sample was 4096 points, i.e. the averaging time equaled about 17.1 min.

The study was carried out in three successive stages in accordance with the longitudinal, vertical, and transverse disposition of the sensor linearly arranged set, relative to the average wind direction. At each stage the experiment was carried out in an automated mode of operation controlled using two personal computers. These computers also recorded and partially processed the data on a real time scale. Thus recorded data have then been subjected to a more detailed analysis and statistical processing.

We have analyzed 35 measurement sessions. For each run the following statistical characteristics were determined: for the longitudinal wind velocity component and temperature we calculated the average values, variances, asymmetry and excess, autocorrelation functions, and auto spectra at each sensor point, and also the mutual correlation functions, spectra of coherence and phase were calculated for the sensors placed at the distance 1–5 m from each other. Besides, based on the data of the weather station we calculated the single-point moments and spectra for the transverse and vertical wind velocity components and the scales of velocity (friction velocity), temperature, specific humidity, length (Obukhov scale), vertical turbulent flux of the momentum, water vapor, explicit and latent heat were also calculated.

Although the question on similarity of temperature fluctuations to the wind ones has been widely discussed by Byzova N.L. , Ivanov V.N. , and Garger E.K., 1989) at present an assumption about the identical nature of the turbulent heat and momentum exchange in the surface layer of the atmosphere is a hypothesis and needs for the further experimental tests. In this paper we, however, are limited by a comparative analysis of the behavior of spatiotemporal correlation functions and coherence spectra of fluctuations of the temperature and wind velocity components.

The range of variation of the thermal stratification conditions during the experiment, in terms of the parameter z/L (where L is the Obukhov scale, z is the observation altitude), was quite broad, i.e., the state of the surface layer changed from a very stable state (1 class, by Terner)

at night to a very unstable one (7 class) during day-time. Change of the surface layer state is shown in Fig. 16.

As known (Lumley J.L. and Panofsky H.A., 1964), the temperature fluctuations arise in the atmosphere only if the height stratification of the potential temperature occurs. According to (Lumley J.L. and Panofsky H.A., 1964) no temperature fluctuations are generated in the presence of adiabatic gradient of the potential temperature (neutral stratification conditions). When the vertical temperature gradient deviates from the adiabatic one, vertical motion of the elementary volumes of air by fluctuations of the vertical velocity leads to local temperature fluctuations. Reduction of the variance of these fluctuations σ_t^2 to a dimensionless form is done using the temperature scale T^* determined by the equality $\langle t'w' \rangle = -u^*T^*$, where t' and w' are the fluctuations of temperature and wind velocity vertical component, u^* is the friction velocity.

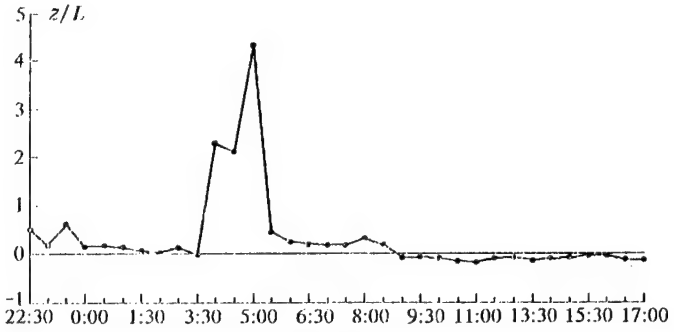

FIG. 16.

Figure 17 shows the normalized variance of temperature fluctuations as a function of stability according to data from our measurements. One can see that at the stratification close to neutral the magnitude $\sigma_t / |T^*|$ increases. On the whole the dependence presented well agrees with the theoretical statements and known experimental data.

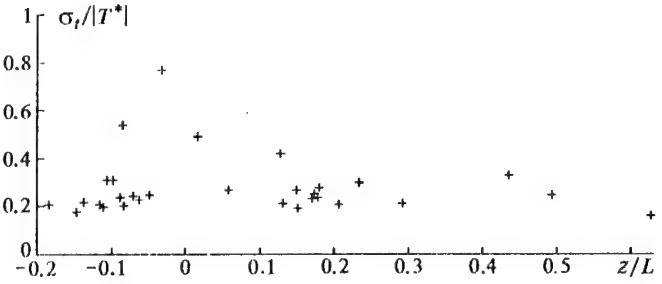

FIG. 17.

In (Byzova N.L. , Ivanov V.N. , and Garger E.K., 1989) the similarity principle of temperature fluctuations spectra to wind ones is used. However, there is a difference between these spectra connected with the temperature field may not be stretched itself, but it is transferred by the velocity field. In this case the inertia intervals of these two fields overlap partially, but their coincidence is not necessary (Lumley J.L. and Panofsky H.A., 1964). A possible cause of the difference in temperature and wind velocity spectra may be different behaviors of the turbulent exchange coefficients. At present the difference between the turbulent exchange coefficients depending on the stratification is established quite reliably (Newstad F.T.M. and Van Dop H., 1983). In accordance with the Monin–Obukhov similarity theory in the atmospheric surface layer the ratio between the turbulent exchange coefficients α for the heat K_h and momentum K_m is a function of the stability parameter (dimensionless height) $\xi = z/L$: $\alpha = K_h/K_m = \varphi_m(\xi)/\varphi_h(\xi)$, but it is impossible to determine the functions $\varphi_m(\xi)$ and $\varphi_h(\xi)$ with the similarity theory. To do this one needs for corresponding experimental data. In accordance with the results of numerous measurements of the velocity and temperature

profiles, including the laboratory conditions, the value α was found to be 1.16 at $\xi = 0$. Since, by definition, $\varphi_m(0) = 1$ the function $\varphi_h(0) = 0.86$. However, many authors consider that the relations of φ_m and φ_h to ξ obtained by processing of the experimental data requires further refinement (Newstad F.T.M. and Van Dop H., 1985).

Examples of the temperature and wind velocity fluctuation spectra normalized to the variance we have obtained under conditions of stable, neutral, and unstable stratification are presented in Figs. 18, 19, and 20, respectively. Unfortunately for the stable and neutral states of the surface layer stratification the intensity of turbulent fluctuations was very weak, and the spectral characteristics were close to those of pure noise. At large z/L values the short-duration sporadic manifestations of the turbulence lasting 0.5–5 min were observed in certain cases only. Since the averaging time was about 17 min this led to a disturbance of the stationary conditions during the sampling time. It is clear from Figs. 18 and 19 that the inertia interval in spectra is small, and a rise in the spectral curves in the high frequency region is explained by noise. These results agree with the conclusions from Byzova N.L. , Ivanov V.N. , and Garger E.K., 1989 that in the night surface layer the turbulence is intermittent. Also these results agree with the data of similar experiments described by Newstad F.T.M. and Van Dop H., 1985, where it was shown that at $Ri \approx 0.2$ in some observational series the slope of the dimensionless spectra multiplied by the frequency was close to zero and had the values from −1.2 to −2.5 in the other ones.

Measurements of temperature fluctuations under unstable stratification showed that almost all disturbance energy concentrates near the spectral maximum that is clearly observed in the low frequency region, and in the inertia interval the spectra really obey the "2 thirds law" (see Fig. 20).

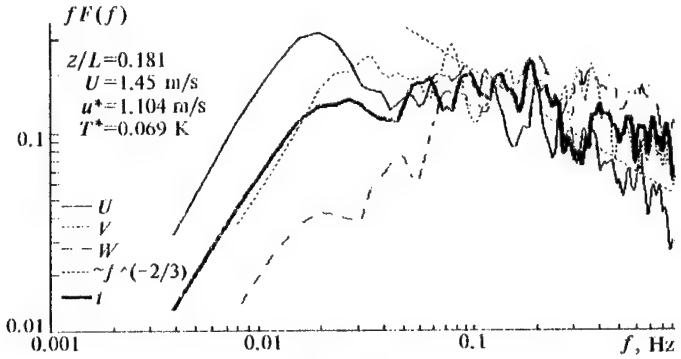

FIG. 18.

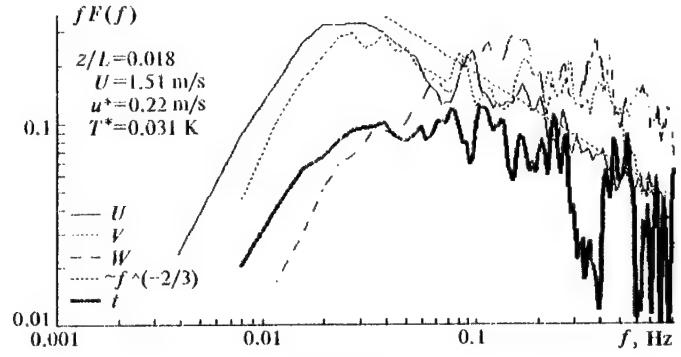

FIG. 19.

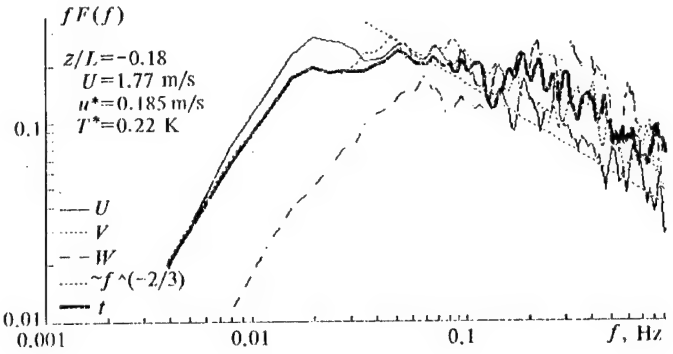

FIG. 20.

It is known (Newstad F.T.M. and Van Dop H., 1985, Byzova N.L. , Ivanov V.N. , and Garger E.K., 1989, Lumley J.L. and Panofsky H.A., 1964) that in the surface layer the turbulence is essentially anisotropic. Let us consider some manifestations of the anisotropy in the example of spatiotemporal correlation functions of fluctuations of the longitudinal wind velocity component and temperature measured under the condition of unstable stratification, which are shown in Figs. 21, 22, and 23 for the longitudinal, transverse, and vertical separations between the sensor points of the acoustic meters, respectively.

The most slow drop of the correlation maxima takes place in the longitudinal direction both for the velocity fluctuations (the curves *1*–*4*) and for temperature ones (the curves *1'*–*4'*). Moreover when the spatial separation of points increases (the curves *1* to *4* correspond to the separations 1, 3, 4, and 5 m), the natural decrease of the correlation maxima and rise in the time delay of their location are observed, i.e. a satisfactory fulfillment of the hypothesis of "frozen" turbulence takes place in this direction.

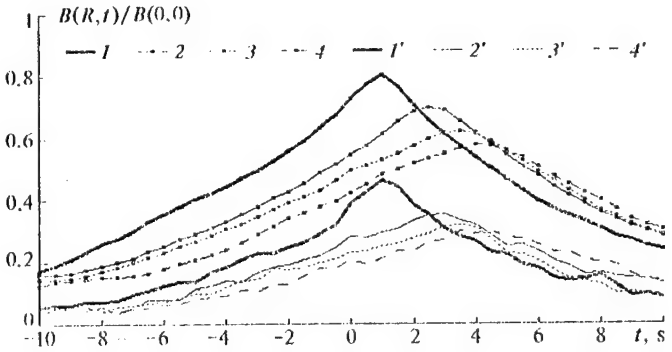

FIG. 21.

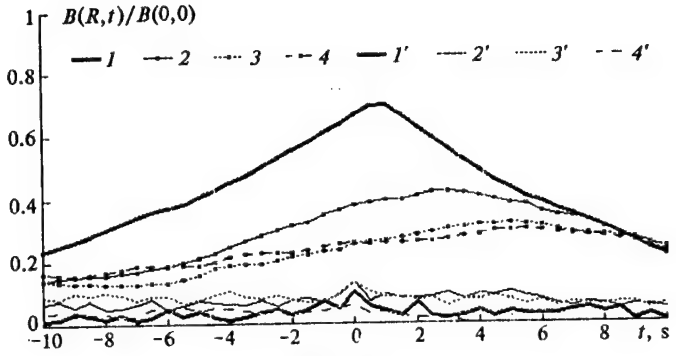

FIG. 22.

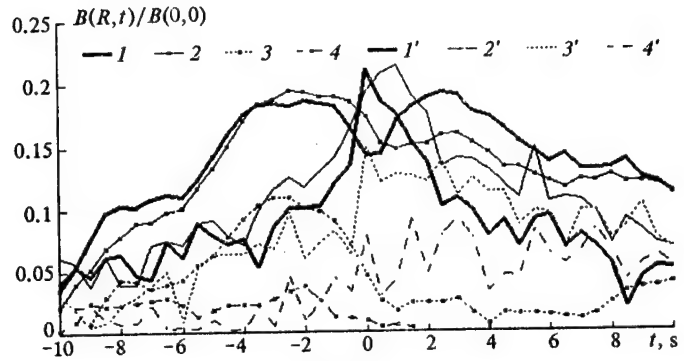

FIG. 23.

In the transverse direction the drop of the wind fluctuation correlation occurs considerably more quickly then in the longitudinal direction, and the level of the temperature correlation is considerably lower then for wind. Moreover, if for fluctuations of the longitudinal velocity a correspondence of the maximum values and their temporal delays to the values of spatial separations is still traced, then for the temperature fluctuations this dependence is broken, and a shift of maxima is absent at all.

As is clear from Fig. 23 for the separation of meters in the vertical direction (here the curves *1*–*4* correspond to the separations 1, 2, 3, and 4 m) the correlation of the longitudinal velocity fluctuations was most low. However, here a decrease of the statistical relation of fluctuations is traced as far as the difference of heights increases. The peculiarity of the fluctuation correlation with the vertical separation is that the correlation maximum between the levels (for example, the levels at 2 and 3 m apart – the curves *2* and *3*, respectively) is observed not for the positive time delay, as for the cases of the longitudinal and transverse separations, but for the negative ones, i.e. when the observations at the upper level precede to observations at the lower level. Such a shift of the cross-correlation function maximum in accordance to Lumley J.L. and Panofsky H.A., 1964 means a slope of turbulent eddies towards the average motion due to their interaction with the positive (upward) gradient of the average velocity.

It is interesting, that when the distance between the levels is not too large (R = 1 m, the curve *1*), in the given realization a presence of two weakly pronounced local maxima with the time delay opposite in sign is observed. It is possible, that the right-hand side maximum with the positive delay is connected with the vertical component of the average wind velocity caused by the air flows from heated underlying surface occurs in the surface layer under conditions of unstable stratification. It must be so, that the regular vertical transfer of inhomogeneities by this component leads to appearance of maximum at a positive delay. Since this component is small (in this case $\langle w \rangle$ = 0.1 m/s) its influence on the maximum shift is detected only for close levels, where the influence of corresponding difference of the longitudinal velocities caused by the presence of the logarithmic profile is less important. As one can see from Fig. 23 the right-hand side maximum practically disappears at the separation R = 2 m already (owing to

the influence of ordinary processes of the evolution of inhomogeneities of the velocity and turbulent mixing).

As regards the temperature fluctuations although the correlation is also low, as in the case of the transverse separation, one can notice, that the maximum of functions is reached not at negative time shift, as for the longitudinal velocity fluctuations, but for a positive one, i.e. by the transfer of temperature inhomogeneities upwards by the average vertical component of the wind velocity.

On the whole Figures 21–23 show that during the measurements under moderately unstable stratification conditions of the surface layer the velocity vortexes were most strongly stretched along the direction of average motion. Typical dimension of the vortexes in the transverse direction was smaller than in the longitudinal one, but it was considerably larger than in the vertical direction. Spatial correlation of the temperature inhomogeneities drops most slowly for the horizontal position of the sensors linear array along the average wind direction also. However, in the transverse and vertical directions the behavior of the correlation functions of the temperature fluctuations essentially differs from that of corresponding correlation functions of the longitudinal velocity fluctuations. All this shows that the essential distinctions in the structure of turbulent fields of wind velocity and temperature which are expressed in different manifestations of the spatial anisotropy of their statistical characteristics.

To study the detailed structure of turbulent fields of the velocity and temperature information on the degree of statistical relation of fluctuations in different spatial points for the specific values of frequency is of certain interest. Such information is in the coherence functions

$$\mathrm{Coh}^i(f, R_j) = [\mathrm{Co}^2(f) + Q^2(f)] \,/\, [F_A^i(f)\ F_B^i(f)], \quad i, j = 1, 2, 3, \tag{6.1}$$

where f is the frequency; $F_A^i(f)$ and $F_B^i(f)$ are the power spectra at the points A and B, respectively; R_j is the distance between the points A and B; $\mathrm{Co}(f)$ is the cospectrum, and $Q(f)$ is the quadrature spectrum; indices $i, j = 1, 2, 3$ mean the longitudinal, transversal, and vertical wind components and longitudinal, transversal, and vertical disposition of the sensor array relative to the average wind direction, respectively.

The coherence (6.1) is a statistical characteristic determining the contribution of fluctuations of different frequencies into the correlation between the fluctuations of meteorological quantities at two spatially separated points. As applied to the wind velocity the coherence can be treated as a measure of the velocity vortex stability.

Figures 24 and 25 show the behavior of the coherence functions for the horizontal velocity components (curves *1* and *2*) and for temperature (curves *1'* and *2'*) measured for the separations between the observation points R = 1 m (curves *1* and *1'*) and R = 5 m (curves *2* and *2'*) along the average wind velocity direction for conditions of unstable and stable stratifications, respectively. One can see from Fig. 24 high values of the coherence between fluctuations at the points of sensor locations in the low frequency region for unstable stratification, as it could be expected from the known conceptions of the turbulent motion in the near surface layer (Lumley J.L. and Panofsky H.A.,1964).

When the frequency increases, i.e. when going to smaller scales of turbulent inhomogeneities, a decrease in the coherence takes place as in the case when a distance between the measurement points increases. In this case obvious distinctions in the behavior of temperature and wind fluctuations are not revealed in the case when the correlation functions at the longitudinal separation of sensors.

When the stratification is stable (Fig. 25), a drop of the coherence with increasing frequency and distance between the points is more quick than it occurs under unstable one. This fact can be explained by a general decrease in the turbulence energy due to the buoyancy Archemedes force and corresponding decrease of all scales (Newstad F.T.M. and Van Dop H., 1985). Moreover, a certain distinction in the behavior of temperature and wind coherence is observed

in the low frequency region. If for the longitudinal wind velocity component the coherence increases with a decrease in the frequency as in the case for an unstable stratification, then the temperature fluctuation coherence, when going to larger spatial scales first reaches its maximum value and then begins to decrease. The presence of such a low-frequency maximum in the coherence spectra of temperature fluctuations means that the main contribution into their spatial correlation is introduced by the inhomogeneities with the scale, which is smaller than the typical scale of the longitudinal velocity.

If one takes into account that the mechanism of temperature fluctuation generation for the stratification different from neutral is, on the whole, caused by the vertical velocity component fluctuations, then such a scale must be certain typical size of the turbulent inhomogeneities along the vertical direction. Under stable stratification conditions the turbulent eddies of velocity are compressed along the vertical direction by the buoyancy force.
Thus, the aforesaid distinctions of the turbulent exchange coefficients and spatial anisotropy of the turbulent inhomogeneities is also a factor causing the difference in the behavior of spectral characteristics of the longitudinal velocity component and temperature in the low-frequency region. At higher frequency time scales are smaller and the eddies are more isotropic.

For a theoretical generalization of the experimental data of wind coherence the following model representations (Mazurin V.P., 1983) are often used

$$\mathrm{Coh}^i(f, R_j) = \exp(-K_j^i n_j) \quad i, j = 1, 2, 3, \tag{6.2}$$

where $n_j = f R_j / V_i$ is the dimensionless frequency; K_j^i is the attenuation parameter. The curves *1a* and *2a* in Figs. 24 and 25 are the exponential approximation of the corresponding experimental coherence functions of the longitudinal velocity component. The values of attenuation coefficients obtained qualitatively obey the relationships determined in Mazurin V.P.,1983) based on a comparison of a large number of the experimental investigations performed by different authors in different sites.

According to the conclusions from Mazurin V.P., 1983, under unstable stratification no noticeable dependence of K_1^1 on R exists. Really, the values of attenuation parameter K_1^1 for $R = 1$ and 5 m obtained from our measurements have close magnitudes of 5.03 and 4.01, respectively (the curves *1a* and *2a* in Fig. 24). At the same time, under stable stratification (curves *1a* and *2a* in Fig. 25) these parameters are 4.92 and 10.1 for the same separations. These values well agree with the conclusions from Mazurin V.P., 1983 that the growth of K_1^1 is observed at the increase of R under stable stratification. Moreover, if at large separations ($R = 5$) the growth of K_1^1 is observed when the stability increases (the values 4.92 and 10.1 for the unstable and stable conditions), at small separations ($R = 1$) the attenuation parameter can even decrease (the values 5.03 and 4.01, respectively). Such a dependence agrees with the results of some investigations described in Mazurin V.P., 1983.

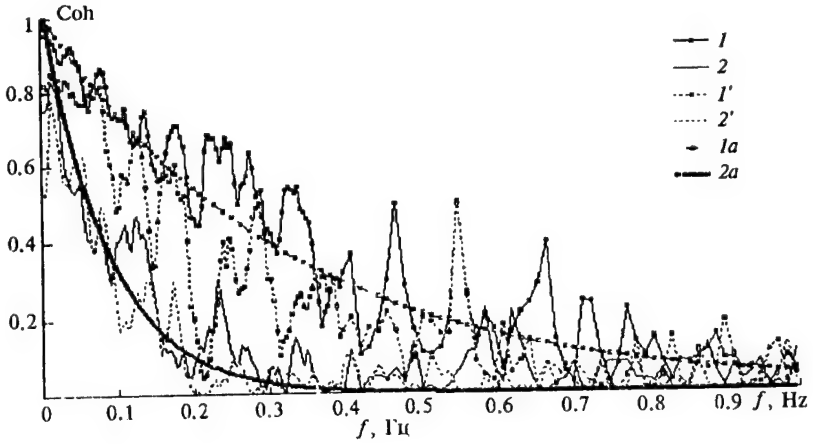

FIG. 24

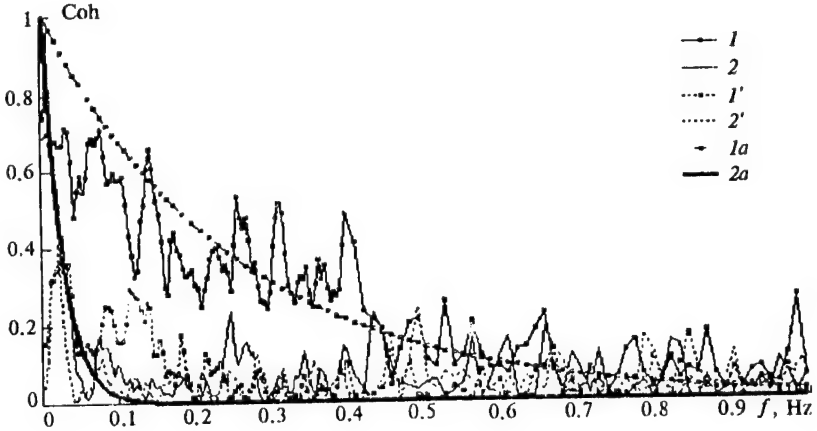

FIG. 25

To obtain a more detailed quantitative conclusions about the influence of the stability conditions in the surface layer on the degree of the turbulence spatial anisotropy more long experiments are needed allowing for the influence of a set of additional factors like the boundary layer height, underlying surface roughness, etc. Nevertheless, it is obvious from the analysis presented that similar complex automated measurements are a good possibility to study the surface layer turbulence where the synchronous data sampling is needed for a large number of hydrometeorological parameters. The cases of weak and intermittent turbulence[5] require additional study. A positive aspect applying the acoustic meters[2] from this point of view is high accuracy and high rate of recording velocity and temperature fluctuations allowing the fine effects in structure of turbulent fields to be investigated. The data obtained can be used for theoretical generalization and identification of new relationships of the behavior of small-scale turbulence in the atmospheric surface layer.

7. STRUCTURE CHARACTERISTIC FOR TEMPERATURE FLUCTUATIONS AND THE OUTER SCALE OF ATMOSPHERIC TURBULENCE RECONSTRUCTED FROM THE DATA OF ACOUSTIC SOUNDING

Nowadays acoustic radars (sodars) are widely used to measure the profiles of structure characteristics for temperature fluctuations in the atmospheric boundary layer. However, a comparison of sodar data with *in situ* measurements shows that the standard deviation of sodar data reaches 40% at altitudes 30–500 m. Their maximum discrepancy may reach a factor of 2–5. We believe that a possible reason for the discrepancy is neglect of the turbulent attenuation of a sodar signal when it propagates to a sounded volume and back to a receiver. In the present report, the interpretation of sodar data is performed with the use of an iterative algorithm (Krasnenko N.P., Shamanaeva L.G., 1997) considering the turbulent signal attenuation. This allows the vertical profiles of the outer scale of atmospheric turbulence to be obtained.

The outer scale of turbulence plays an important role in the theory of turbulence, because it defines the low-frequency boundary of the inertial subrange in the spectra of temperature and wind velocity fluctuations (Kolmogorov A.N., 1941). Knowledge of L_0 is necessary for estimating the turbulent attenuation of a sound wave (Baikalova R.A. et al., 1988). Nevertheless, the vertical profiles of L_0 have never been measured in the atmospheric boundary layer, although Sazarin M., 1990 point out their strong dependence on local orography.

In the present report, we discuss the vertical profiles of the structure characteristic for temperature fluctuations C_T^2 and the outer scale of atmospheric turbulence L_0 measured with the Zvuk–2 three-channel Doppler sodar. Sodar specifications are given below.

Vertical sensing range, m 40–700
Operating frequency f, Hz 1650–1850

Electrical transmitted power P_0, W 65
Pulse repetition period Δt, s 4, 6, 12
Pulse duration τ, ms 150
Effective transceiving antenna area A_{eff}, m^2 ..... 0.5
Efficiency of conversion of electrical power into acoustic power and *vice versa*, $\gamma_1 = \gamma_2$ 0.1

The structure characteristic of temperature fluctuations is calculated by the formula

$$C_T^{2(j)}(z_i) = \frac{2.7 \cdot 10^2 \lambda^{1/3} T^2 P(z_i) z_i^2}{\gamma_1 \gamma_2 P_0 c A_{eff} \tau L^{(j-1)}(z_i)}, \qquad (7.1)$$

where j is the iteration number, $j = 1,..., M$; z_i is the current altitude of the sounded volume, $z_i = i\Delta z$, $\Delta z = c\tau/2$ is the altitude resolution of the sodar, $i = i_0, i_0 + 1,..., N$; i_0 specifies the minimum sounding altitude $z_0 = i_0 \Delta z$, N specifies the maximum sounding altitude and is equal to the number of range gates in the realization; c is the sound speed in air, $c = 20.05\sqrt{T}$; T is the surface air temperature; $\lambda = c/f$ is the acoustic radiation wavelength; $P(z_i)$ is the power of the acoustic signal coming from the altitude z_i;

$$L^{(j)}(z_i) = L_{abs}(z_i)\, L_{turb}^{(j)}(z_i) \qquad (7.2)$$

is the attenuation factor considering the signal attenuation on the propagation path to the sounded volume and back to the receiver caused by the classical and molecular absorption $L_{abs}(z_i)$ and by the turbulent attenuation $L_{turb}^{(j)}(z_i)$ due to scattering by temperature and wind velocity fluctuations.

The first iteration $C_T^{2(1)}(z)$ was calculated from Eq. (7.1) without turbulent attenuation for

$$L^{(0)}(z_i) = L_{abs}(z_i) = \exp\{-2\,(\beta_{cl} + \beta_{mol})\, z_i\}. \tag{7.3}$$

In so doing, the classical and molecular absorption coefficients were calculated by the formulas (Neff W.D., 1975)

$$\beta_{cl}(f) = 4.02\cdot10^{-11}\, f^2,\ [m^{-1}]\ , \tag{7.4}$$

$$\beta_{mol}(f, t, u) = \frac{\beta_{max}}{304.8}\left[(0.18 f_k)^2 + \left(\frac{2 f_k^2}{1+f_k}\right)^2\right]^{1/2},\ [m^{-1}]\ , \tag{7.5}$$

where $f_k = f/f_m$, f_m is the frequency at which the maximum absorption occurs at the given temperature t[°C], pressure p[mbar], and relative humidity u[%], determined from the formula

$$f_m = (10 + 6600\, h + 444000\, h^2)\, p_1 / t_1^{0.8}\ . \tag{7.6}$$

Here, the normalized pressure $p_1 = p/1014$, $t_1 = (1.8t + 492)/519$, and the parameter $h = e_1\cdot100/p_1$ depends on the water vapor pressure e_1 in the atmosphere which is given by the formula (Komarov V.S., 1971)

$$e_1 = 0.0611107\cdot10^{M_1}\cdot u \tag{7.7}$$

with

$$M_1 = 7.63\, t/(241.9 + t)\ . \tag{7.8}$$

Then the parameter β_{max} in Eq. (7.5) is calculated from the relation

$$\beta_{max} = 0.0018\ t_1^{-2.5}\ \exp\{7.77\ (1 - t_1^{-1})\}\ . \tag{7.9}$$

The second and the next iterations of C_T^2 were calculated considering the turbulent attenuation. The turbulent attenuation factor in Eq. (7.2) (for the jth iteration) was calculated by the formula

$$L_{turb}^{(j)}(z_i) = \exp\left\{-2\Delta z \sum_{i=1}^{N}\left[\beta_V^{(j)}(z_i) + \beta_T^{(j)}(z_i)\right]\right\}. \tag{7.10}$$

Here, the coefficients of scattering by the temperature and wind velocity fluctuations were calculated by the formulas

$$\beta_V^{(j)}(z_i) = 9.545\ \frac{C_V^2(z_i)}{c^2}\frac{\left[L_0^{(j)}(z_i)\right]^{5/3}}{\lambda^2}\ , \tag{7.11}$$

$$\beta_T^{(j)}(z_i) = 0.3596\ \frac{C_T^{2(j)}(z_i)}{T^2}\frac{\left[L_0^{(j)}(z_i)\right]^{5/3}}{\lambda^2}\ , \tag{7.12}$$

derived in (Baikalova R.A. et al., 1988) for $L_0^2 \gg \lambda^2$, which is satisfied in our case (λ = 20 cm). The jth iteration of C_T^2 entering Eq. (7.12) was calculated by Eq. (7.1).

The outer scale of atmospheric turbulence and the structure characteristic of wind velocity fluctuations were determined as follows.

The structure characteristics of the wind velocity fluctuations were determined by averaging of the instantaneous wind velocity components $V_{x_k}(z_i)$, $V_{y_k}(z_i)$, and $V_{z_k}(z_i)$ measured by the Zvuk–2 sodar

$$C_V^2(z_i) = (\Delta t\sqrt{V_{xav}^2(z_i)+V_{yav}^2(z_i)+V_{zav}^2(z_i)})^{-2/3}\ \frac{1}{K-1}\sum_{k=1}^{K-1}[V_k(z_i) - V_{k+1}(z_i)]^2, \tag{7.13}$$

where $\Delta t = 12$ s is the sound pulse repetition period, $M = 50$ is the number of pulses in a measurement series,

$$V_{x\,av}(z_i) = \frac{1}{K}\sum_{k=1}^{K} V_{x_k}(z_i),\ V_{y\,av}(z_i) = \frac{1}{K}\sum_{k=1}^{K} V_{y_k}(z_i),$$

$$V_{z\,av}(z_i) = \frac{1}{K}\sum_{k=1}^{K} V_{z_k}(z_i) \tag{7.14}$$

are the components of the wind velocity averaged over the period $K\Delta t$, and

$$V_k(z_i) = \frac{V_{xk}(z_i)\cdot V_{x\,av}(z_i) + V_{yk}(z_i)\cdot V_{y\,av}(z_i) + V_{zk}(z_i)\cdot V_{z\,av}(z_i)}{\sqrt{V_{xav}^2(z_i)+V_{yav}^2(z_i)+V_{zav}^2(z_i)}}. \tag{7.15}$$

Because in our experiment we measured only the wind velocity components averaged over 10-min intervals, C_V^2 was approximated by the relation

$$C_V^2(z_i) = C_{V_0}(0.04 + 0.33\ z_i^{-2/3}) \tag{7.16}$$

suggested in (Brown E.H.and Clifford S.F., 1976) for the daytime convection. The parameter C_{V_0} was determined from the data of *in situ* measurements performed by micropulsation sensors placed 17 m above the ground.

The outer scale of atmospheric turbulence was estimated as follows. At visible wavelengths, Tatarskii V.I., 1961 derived the expression for the structure characteristic of the refractive index

$$C_n^2(z_i) = 2.8\ M(z)\ L_0^{4/3}(z), \tag{7.17}$$

where $M(z)$ is the potential refractive index gradient related with the gradient of the potential temperature logarithm by the formula

$$M(z) = -78\cdot 10^6\ \frac{\rho(z)}{T(z)}\frac{\delta \ln\theta(z)}{\delta z}. \tag{7.18}$$

In its turn, the potential temperature is defined by the air temperature and pressure

$$\theta(z) = T(z)\ [1000/p(z)]^{0.286}. \tag{7.19}$$

According to the formula (Coulman C.E. et al., 1988)

$$C_n^2(z) = C_T^2(z)\left[\frac{78\cdot 10^6\,\rho(z)}{T^2(z)}\right]^2, \tag{7.20}$$

the structure characteristic of the refractive index at visible wavelengths is connected with the structure characteristic of the temperature fluctuations, so from Eqs. (7.17)–(7.19) we derive

$$L_0(z) = \left[\frac{C_T^2(z)}{2[\delta\theta/\delta z]^2}\left(\frac{\rho(z)}{1000}\right)^{0.572}\right]^{3/4}. \tag{7.21}$$

For the atmospheric boundary layer at altitudes $40 \le z \le 700$ m, we can take $p(z) \cong 1000$ mbar, $\delta\theta/\delta z \cong \gamma_a$ (see Matveev L.T., 1976), where γ_a is the adiabatic temperature gradient. Finally, for the jth iteration of the outer scale of atmospheric turbulence we obtain

$$L_0^{(j)}(z_i) = [C_T^{2(j)}(z_i)/(2.8\gamma_a^2)]^{3/4}. \tag{7.22}$$

The iterative algorithm of acoustic sounding data processing was constructed in the following way. The structure characteristic of temperature fluctuations was calculated by Eq. (7.1) and the outer scale of atmospheric turbulence – by Eq. (7.22) sequentially for each strobe pulse $i = i_0$, $i_0 + 1$, ..., N. The minimum sounding altitude $z_0 = i_0\Delta z$ was determined by the sodar dead zone and environmental noise level and changed from 66 to 88.5 m as a function of meteorological conditions and surrounding noise level. The maximum sounding altitude changed from 250 to 650 m. For each strobe pulse starting from i_0 the first iteration $C_T^{2(1)}$ was calculated without turbulent attenuation. Then the first iteration of the outer scale of turbulence $L_0^{(1)}$ was calculated by Eq. (7.22). Its value was used to calculate the first iterations of the attenuation coefficients by Eqs. (7.11) and (7.12). It was substituted into Eq. (7.10) to calculate the first iteration of the turbulent attenuation factor which was further substituted into Eq. (7.1) to calculate the second iteration $C_T^{2(2)}(z_i)$, and so on. The iteration process terminated when the number of iterations exceeded 100 or when the next iterations started to diverge.

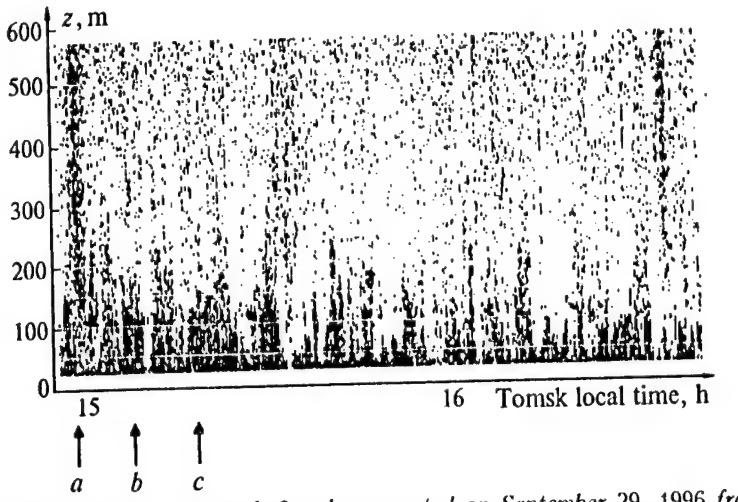

FIG. 26. The facsimile record of the Zvuk–2 sodar operated on September 29, 1996 from 14:55 to 16:47, Tomsk local time. The arrows indicate times of starting of three subsequent runs; their data were processed with the use of the proposed iterative algorithm.

Figure 26 shows the facsimile record of the Zvuk–2 sodar operated on September 29, 1996 under conditions of developed convection. Intensive thermal plumes up to 120–200 m can be seen. The arrows indicate times of starting of three subsequent 10-min runs; the corresponding vertical profiles of C_T^2 are shown in Fig. 27.

For comparison, Fig. 28 shows the vertical profiles of C_T^2 reconstructed from the data of acoustic sounding in the morning under conditions of developing convection. The structure characteristics were normalized to $C_T^2(z_0)$ measured at the minimum sounding altitude. Their numerical values are indicated near the curves.

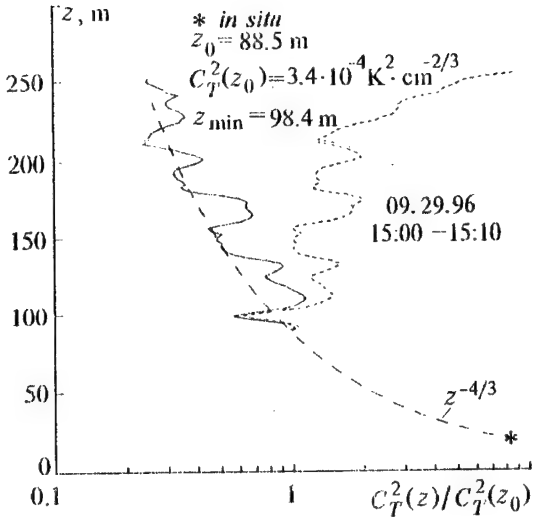

a

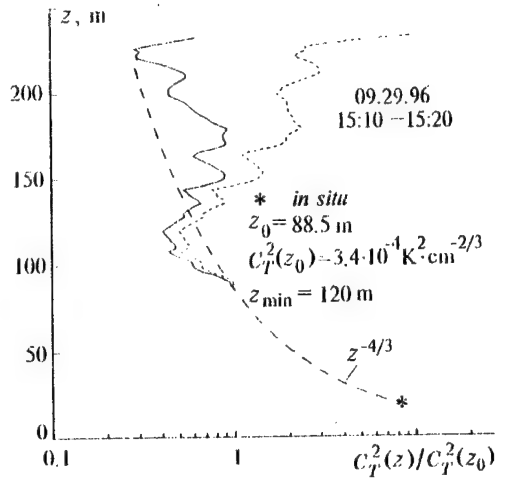

b

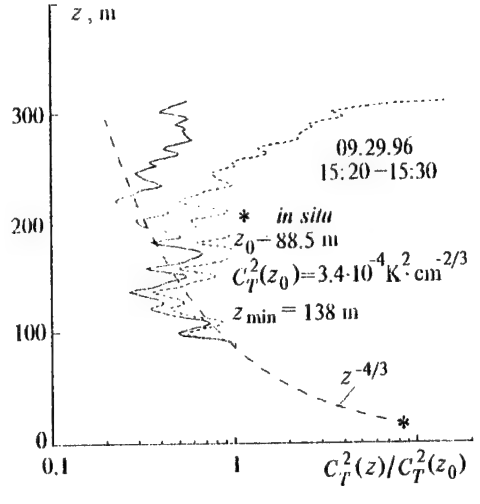

c

FIG. 27. Normalized vertical profiles of C_T^2 for three subsequent runs indicated in Fig. 26.

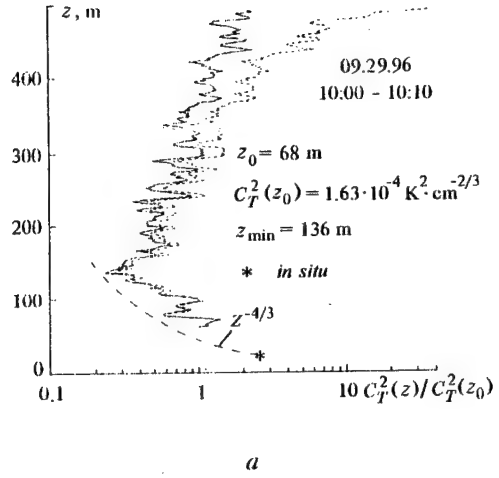

a

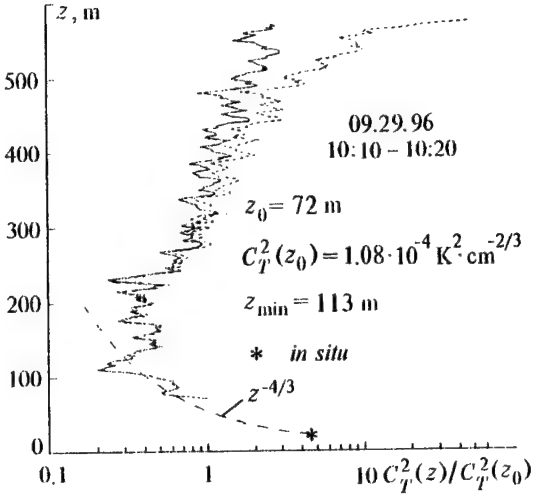

b

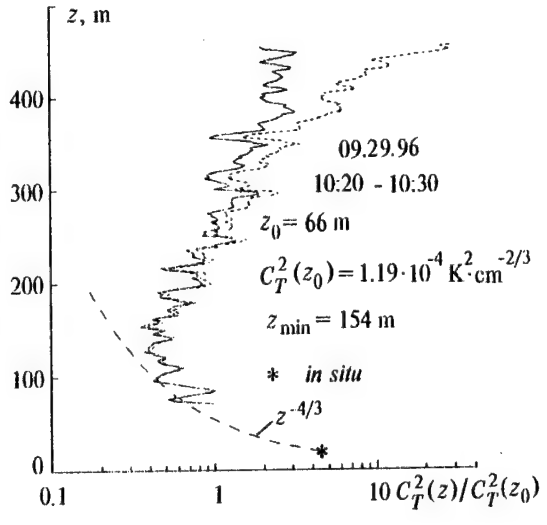

c

FIG. 28. Normalized vertical profiles of C_T^2 for three subsequent 10-min runs under conditions of developing convection.

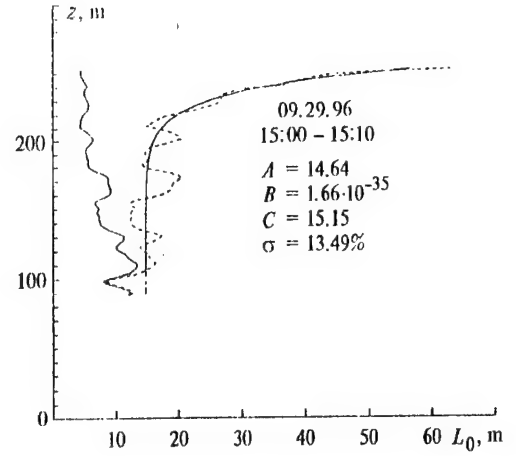

a

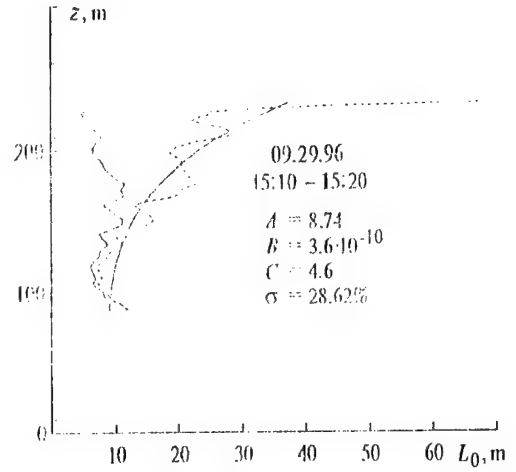

b

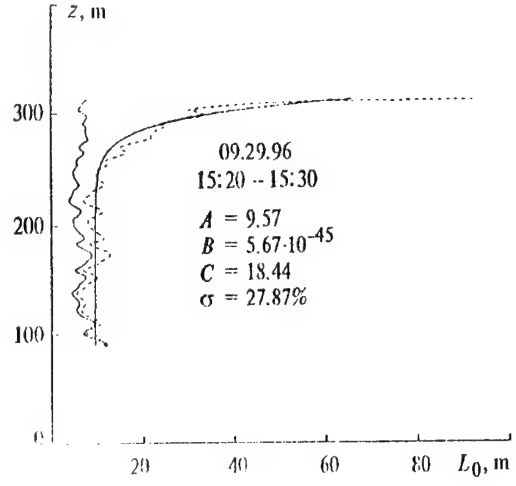

c

FIG. 29. Vertical profiles of the outer scale of atmospheric turbulence for three subsequent runs indicated in Fig. 26. The corresponding vertical profiles of C_T^2 are shown in Fig. 27.

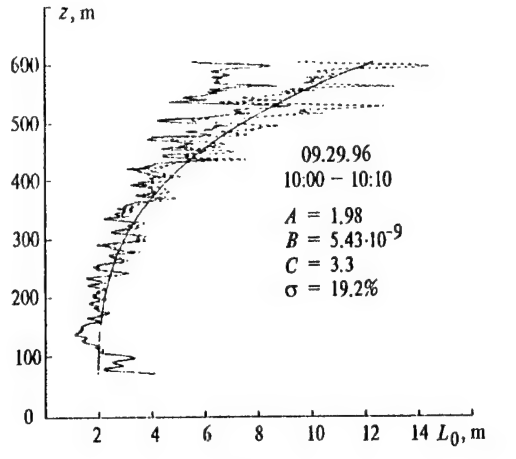

a

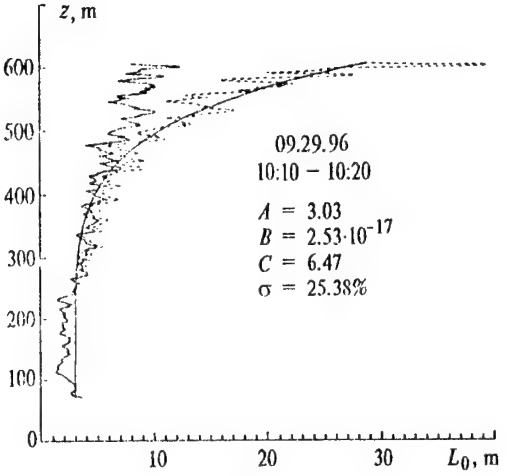

b

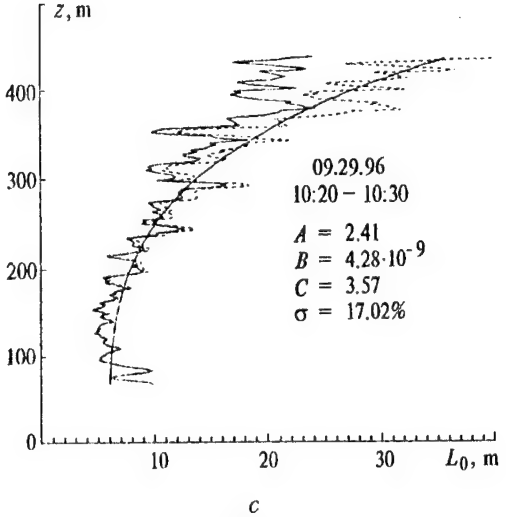

c

FIG. 30. Vertical profiles of the outer scale of atmospheric turbulence for three subsequent 10 min runs on September 29, 1996. The measurements started at 10:00, Tomsk local time, under conditions of developing convection. The corresponding profiles of C_T^2 are shown in Fig. 28.

The solid curves are for the first iteration and the dashed curves are for the last iteration for 5% level of convergence of the algorithm. The long-dashed curve illustrates the dependence $C_T^2(z) \sim z^{-4/3}$ predicted theoretically for convective conditions. All curves reach their minima at z_{min}. Below z_{min}, the behavior of C_T^2 is described well by the theoretically predicted dependence. Above z_{min} C_T^2 increases with the altitude, which was also indicated by Neff W.D., 1975. The asterisks indicate the values of C_T^2 (17 m) calculated from the data of simultaneous measurements with micropulsation sensors.

Considering $z^{-4/3}$ dependence, they agree well with the sodar data.

Figures 29 and 30 show the vertical profiles of L_0 for these runs.

The solid curves show the first iterations and the dashed curves show the last ones. The obtained profiles were approximated by the nonlinear least-squares method using the relation

$$L_0(z) = A + B\, z^C. \tag{7.23}$$

The values of the corresponding coefficients and the rms fitting errors δ are also shown in the figures. The smooth solid curves illustrate this empirical dependence.

As can be seen from Figs. 29 and 30, the outer scale of turbulence increases with the altitude. This agrees with the existing models of the outer scale of atmospheric turbulence reviewed in (Lukin V.P. et al., 1997). Its near-ground values A change from 1.98 to 14.68. According to Lukin V.P. et al., 1997, the effective outer scale of atmospheric turbulence determined by minimization of the integral quadratic discrepancy of the structure functions of the optical wave phase fluctuations corresponding to the model profile of the outer scale $L_0(z)$ and the constant value of the outer scale L_0 lies between 0.68–34.7 m for the lowest intensity of the atmospheric turbulence corresponding to the best conditions of vision through the atmosphere and between 1.31–55.4 m for the highest intensity of the atmospheric turbulence corresponding to the worst conditions of vision through the atmosphere. It should be noted that the data of sodar measurements are within these limits.

Within the 80–140 m altitude range the vertical behavior of the outer scale shown in Fig. 29*b* follows the dependence $L_0(z) = 2\sqrt{z}$. In Figs. 29*a* and *c*, L_0 remains practically unchanged at altitudes up to 150–200 m. From Fig. 30 it is seen that the outer scale of atmospheric turbulence changes quasiperiodically with a period of 10 min, because the vertical profiles of L_0 shown in Figs. 30*a* and *c* are very similar. That is, in analogy with Lukin V.P., 1992, we suggest that 10-min intermittence of atmospheric turbulence (dramatic changes of the low-frequency section of the turbulence spectrum) occurs in the atmosphere.

The fact that in the first run under conditions of developed convection (see Fig. 29) we recorded the most strong echo signals from altitudes up to 550 m has engaged our attention; at that time L_0 = 14.64 m in the lower part of the atmospheric boundary layer (ABL). In the second run, the echo signal was weak and L_0 = 8.74 m in the lower part of the ABL (see Fig. 26). In the third run, the echo signal power increased and L_0 = 9.57 m in the lower part of the ABL.

In conclusion it also should be noted that in the morning under conditions of developing convection we recorded smaller values of L_0, which is in agreement with the experimental data reported in (Emaleev O.N. et al., 1979).

CONCLUSION

The effect of the atmospheric channel on the near-ground propagation of acoustic waves in the atmosphere has been considered. Numerically shown is the influence of the meteorological parameters on audibility of sound in the atmosphere. The structure of the amplitude and phase fluctuations of acoustic waves propagating through the turbulent atmosphere near the ground has been analyzed. Our measurements have shown a significant dependence of the temporal characteristics of the amplitude fluctuations on the angle between the propagation path and the direction of wind velocity vector. Temporal spectra of phase difference fluctuations depended on the wind velocity much weaker than in case of line-of-sight propagation. The structure of the temperature and wind velocity fields and vertical profiles of the outer scale of atmospheric turbulence have been experimentally investigated. The feasibility for model descriptions of the spectral tensor of the wind velocity field fluctuations considered as homogeneous anisotropic turbulence were studied based on the experimental data obtained by us. For the first time, the vertical profiles of the outer scale of atmospheric turbulence have been obtained for the atmospheric boundary layer. Sodar-derived outer scale values agree well with the estimates of the effective outer scale of turbulence by optical methods.

REFERENCES

Abramov N.G., Bogushevich A.Ya., Karpov V.I., Krasnenko N.P., Fomichev A.A., 1994: Possibility of operatively forecasting propagation of acoustic noise in the ground atmospheric layer with the account for meteorological conditions. *Atmospheric and Oceanic Optics*, **7**, 403-413.

Baikalova R.A., Krekov G.M., and Shamanaeva L.G., 1988: J. Acoust. Soc. Am., **83**, No. 4, 1332–1335.

Bochkarev N.N. and Krasnenko N.P., 1986: *Abstracts of Papers at the VIII All-Union Symposium on Laser and Acoustic Wave Propagation in the Atmosphere*, Part II, Tomsk, Russia, 304–308.

Bogushevich A.Ya., Krasnenko N.P., 1993: Operative forecast of acoustic noise propagation along ground surface through atmosphere taking into account meteorological condition. *Proc. INTER-NOISE '93*, Leuven, Belgium, **3**, 1751-1754.

Bogushevich A.Ya., Krasnenko N.P., 1996: Determination of the structure characteristic of acoustic refractive index in the atmospheric boundary layer from the measured pressure level in sound shadow zone. *Sov. Phys. Acoustics,* Russia, **42**, 339-346.

Brown E.H. and Clifford S.F., 1976: J. Acoust. Soc. Am., **60**, No. 4, 788–794.

Brown E.H., Hall F.F., 1978: Advances in atmospheric acoustics. *Rev. Geophys. And Space Phys.*, **16**, 47-110.

Byzova N.L., Ivanov V.N., and Garger E.K., 1986: *Turbulence in the Atmospheric Boundary Layer,* Gidrometeoizdat, Leningrad, 263 pp.

Chernov L.A., 1975: *Waves in Random Media*, Nauka, Moskow, 172 pp.

Coulman C.E., Vernin J., Coquenguiot Y., and Cassia L.L., 1988: *Appl. Opt.* **27**, No. 1, 155–160.

Clifford S.F. and Lataitis R.J., 1983: *J. Acoust. Soc. Am.* **73**, No. 5, 1545–1550.

Daigle G.A., Piercy J.E., and Embleton T.F.W., 1978: *J. Acoust. Soc. Am.* **64**, 622–630.

Diaagle C.A.,1980: *J. Acoust. Soc. Am.* **68**, No. 1, 297-302.

Emaleev O.N., Lukin V.P., Pokasov V.V., and Potanin S.F., 1979: *Abstracts of Reports at the Fifth All-Union Symposium on the Propagation of Laser Radiation through the Atmosphere,* Tomsk, Russia, 144–147.

Harris C.M., 1966: Absorption of sound in air versus humidity and temperature. *J. Acoust. Soc. Am.*, **40**, 148-159.

Hidaka T., Kageyama K., and Masuda S., 1985: *J. Acoust. Soc. Japan* (E) **6**, No. 4, 247–256.

Ingard U., 1953: A review of the influence of meteorological conditions on sound propagation. *J. Acoust. Soc. Am.*, **25**, 405-411.

Kolmogorov A.N., 1941: Dokl. Akad. Nauk SSSR **30**, 229.

Komarov V.S., 1971: *Statistical Structure of the Humidity Field in the Free Atmosphere above the Territory of the USSR* ,Gidrometeoizdat, Leningrad.

Krasnenko N.P. and Shamanaeva L.G., 1997: *Atmos. Oceanic Opt.* **10**, No. 2, 129–131.

Krasnenko N.P. and Shamanaeva L.G., 1997: *Extended Abstracts of Reports at the COST-76 Profiler Workshop 1997*, Engelberg, Vol. II, 318–321.

Krasnenko N.P. and Shamanaeva L.G., 1997: *Abstracts of Reports at the Fourth Symposium on Atmospheric and Oceanic Optics,* Tomsk, Russia, 160–161.

Kristensen L., Lenschow D.H., Kirkegaard P., and Courtney M., 1989: *Boundary-Layer Meteorology* **47**, 149–193.

Lukin V.P., 1992: *Atmos. and Oceanic Opt.* **5**, No. 12, 834–840.

Lukin V.P., 1992: *Atmos. and Oceanic Opt.* **5**, No. 4, 229–242.

Lukin V.P., Nosov E.V., and Fortes B.V., 1997: *Atmos. and Oceanic Opt.* **10**, No. 2, 100–106.

Lumley J.L. and Panofsky H.A., 1964: *The Structure of Atmospheric Turbulence* , Interscience, New York.

Matveev L.T., 1976: *Course of General Meteorology. Atmospheric Physics* , Gidrometeoizdat, Leningrad, 639 pp.

Mazurin V.P., 1983: *Statistical Characteristics of Wind Velocity in Application to Wind Loads,* Issue 2. Gidrometeorologiya, Obninsk, 52 pp.

Neff W.D., 1975: *Report ERL 322–WPL,* **38**, Boulder, 34 pp.

Newstadt F.T.M. and Van Dop H., 1985: eds., *Atmospheric Turbulence and Simulation of Pollutant Dispersal* [Russian translation] , Gidrometeoizdat, Leningrad, 351 pp.

Ostashev V.E., 1992: *Propagation of Sound in Moving Media.* Moskow: Nauka, 208 pp.

Otnes R. and Enokson L., 1982: *Applied Analysis of Time Series* [Russian translation], Mir, Moscow, 428 pp.

Parkin P.H., Scholes W.E., 1965: and *J. Sound Vib.*, No. 2, 353–374.

Patrushev G.Ya. and Rostov A.P., 1994: *Abstracts of Papers at the First Inter-Republic Symposium on Atmospheric and Oceanic Optics,* Part II, Tomsk, Russia, 152–153.

Patrushev G.Ya. and Rostov A.P., 1996: *Akust. Zh.*, Russia, **42**, No. 1, 88–90.

Rostov A.P., 1993: *Atmos. and Oceanic Opt.* **6**, No. 1, 62–64.

Sazarin M., ed., 1990: *VLT Report* No. 60, European Southern Observatory, La Silla, 71 pp.

Tatarskii V.I., 1961: *Wave Propagation in a Turbulent Medium,* McGraw-Hill, New York, 548 pp.

Zilintinkevich S.S., 1970: *Dynamics of the Surface Atmospheric Layer,* Gidrometeoizdat, Leningrad, 290 pp.

LIST OF PUBLICATIONS AND TECHNICAL REPORTS

1. Krasnenko N.P., Afanas'ev A.L., Rostov A.P.,1996: Preliminary results of the experimental study of a model for the spectral tensor of the wind velocity field in the ground atmosphere. *1st Interim Report*, Contract № 68171-96-C-9067, 6 pp.
2. Krasnenko N.P., Rostov A.P., 1997: Anisotropy of temporal spectra of the amplitude fluctuating of a sound wave propagating in a turbulent atmosphere above the ground. *2nd Interim Report*, Contract № 68171-96-C-9067, 6 pp.
3. Krasnenko N.P., Afanas'ev A.L., Rostov A.P.,1997: Experimental verification of a model for the spectral tensor of the wind velocity field. *3rd Interim Report*, Contract № 68171-96-C-9067, 7 pp.
4. Krasnenko N.P., Shamanaeva L.G.,1997: Consideration of the turbulent extinction in the interpretation of sodar measurements of C^2_T. *4th Interim Report*, Contract № 68171-96-C-9067, 5 pp.
5. Krasnenko N.P., Rostov A.P., Rubtsova O.A., 1997: Anisotropy of the amplitude fluctuations of the acoustic waves propagated through the turbulent atmosphere near ground. *5th Interim Report*, Contract № 68171-96-C-9067, 6 pp.
6. Krasnenko N.P., Afanas'ev A.L., Rostov A.P., 1998: Study of statistical properties of the wind and temperature fields in the atmospheric surface layer with ultrasonic sensors. *6th Interim Report*, Contract № 68171-96-C-9067, 9 pp.
7. Krasnenko N.P., Shamanaeva L.G., 1998: Structure characteristics for temperature fluctuations and the outer scale of atmospheric turbulence reconstructed from the data of acoustic sounding. *7th Interim Report*, Contract № 68171-96-C-9067, 10 pp.
8. Krasnenko N.P., Shamanaeva L.G., 1997: Consideration of the turbulent extinction in the interpretation of sodar measurements of C^2_T. *Extended Abstracts COST-76 Profiler Workshop 1997*, Engelberg, Switzerland, v.2, p. 318-321.
9. Krasnenko N.P., Shamanaeva L.G., 1998: Structure parameter for temperature fluctuations and outer scale of turbulence reconstructed from the data of acoustic sounding. *Atmos. and Oceanic Optics*, 11, No.1, p.60-65.
10. Bogushevich A., Krasnenko N., 1998: Influence of the atmospheric channel on the sound propagation above the ground surface. *Proc. 9th Int. Symposium on Acoustic Remote Sensing of the Atmosphere and Oceans*, Vienna, Austria, p. 19-22.
11. Krasnenko N.P., Shamanaeva L.G., 1998: Sodar derived vertical profiles of the structural characteristics of temperature fluctuations and the outer scale of turbulence. *Proc. 9th Int. Symposium on Acoustic Remote Sensing of the Atmosphere and Oceans*, Vienna, Austria, p. 223-226.
12. Krasnenko N.P., Shamanaeva L. G., 1998: Sodar measurements of the structural characteristic for temperature fluctuations and the outer scale of turbulence. *Meteorologische Zeitchrift*, Switzerland, in print.

LIST OF INVESTIGATORS

1. Krasnenko N.P. – Principal Investigator
2. Afanas'ev A.L. – section 5, 6; Interim Reports 1, 3, 6
3. Bogushevich A.Ya. – section 2
4. Rostov A.P. – section 3, 5, 6; Interim Report 1, 2, 3, 5, 6
5. Rubtsova O.A. – section 3; Interim Report 5
6. Shamanaeva L.G. – section 7; Interim Reports 4, 7